NAVAL POSTGRADUATE SCHOOL

MONTEREY, CALIFORNIA

THESIS

NUMERICAL SIMULATION OF GROUND COUPLING OF LOW YIELD NUCLEAR DETONATION

by

Brian Holloway

June 2010

Thesis Advisor: Craig Smith
Second Reader: Lew Glenn

Approved for public release; distribution is unlimited

THIS PAGE INTENTIONALLY LEFT BLANK

REPORT DOCUMENTATION PAGE		Form Approved OMB No. 0704-0188

1. AGENCY USE ONLY *(Leave blank)*	2. REPORT DATE	3. REPORT TYPE AND DATES COVERED
	June 2010	Master's Thesis

4. TITLE AND SUBTITLE: Numerical Simulation of Ground Coupling of Low Yield Nuclear Detonation	5. FUNDING NUMBERS
6. AUTHOR(S) Holloway, Brian C.	
7. PERFORMING ORGANIZATION NAME(S) AND ADDRESS(ES) Naval Postgraduate School Monterey, CA 93943-5000	8. PERFORMING ORGANIZATION REPORT NUMBER
9. SPONSORING /MONITORING AGENCY NAME(S) AND ADDRESS(ES) Lawrence Livermore National Laboratory 7000 East Avenue Livermore, CA 94550	10. SPONSORING/MONITORING AGENCY REPORT NUMBER

11. SUPPLEMENTARY NOTES The views expressed in this thesis are those of the author and do not reflect the official policy or position of the Department of Defense or the U.S. Government. IRB Protocol number _____.

12a. DISTRIBUTION / AVAILABILITY STATEMENT	12b. DISTRIBUTION CODE
Approved for public release; distribution is unlimited	

13. ABSTRACT (maximum 200 words)

Without nuclear testing, advanced simulation and experimental facilities, such as the National Ignition Facility (NIF), are essential to assuring safety, reliability, and effectiveness of the nuclear force; these capabilities are invaluable to the nation's Stockpile Stewardship Program (SSP). A significant information gap exists in the hydrodynamic response to nuclear detonations that occur near the earth's surface. Numerical simulation methods were used to evaluate the hydrodynamic response of earth-like materials and to develop the energy coupling/partitioning curve for low yield nuclear detonations close to the earth's surface. Using LLNL's supercomputers and GEODYN hydrodynamic code, the properties of stress, pressure, and energy were evaluated for twelve simulated 2.5kT detonations; six above the surface and six below the surface. The results indicate stronger air blasts for detonations above or near the surface and that energy coupling into the ground changes rapidly with detonation location over a very small range between the above-ground and below-ground interface. This work serves to provide a baseline model to evaluate stress, pressure, and energy in relation to nuclear yield close to the earth's surface. The results support a better understanding of the physics of near-surface detonations and also assist in planning future experimental work at NIF.

14. SUBJECT TERMS National Ignition Facility, GEODYN, Ground Coupling, Coupling Curve, Surface Nuclear Detonation	15. NUMBER OF PAGES 93
	16. PRICE CODE

17. SECURITY CLASSIFICATION OF REPORT	18. SECURITY CLASSIFICATION OF THIS PAGE	19. SECURITY CLASSIFICATION OF ABSTRACT	20. LIMITATION OF ABSTRACT
Unclassified	Unclassified	Unclassified	UU

NSN 7540-01-280-5500

Standard Form 298 (Rev. 8-98)
Prescribed by ANSI Std. Z39.18

THIS PAGE INTENTIONALLY LEFT BLANK

Approved for public release; distribution is unlimited

NUMERICAL SIMULATION OF GROUND COUPLING OF LOW YIELD NUCLEAR DETONATION

Brian C. Holloway
Captain, United States Army
B.S., Morgan State University, 2001

Submitted in partial fulfillment of the
requirements for the degree of

MASTER OF SCIENCE IN APPLIED PHYSICS

from the

NAVAL POSTGRADUATE SCHOOL
June 2010

Author: Brian Holloway

Approved by: Craig Smith
Thesis Advisor

Lew Glenn
Second Reader

Andres Larraza
Chairman, Department of Physics

THIS PAGE INTENTIONALLY LEFT BLANK

ABSTRACT

Without nuclear testing, advanced simulation and experimental facilities, such as the National Ignition Facility (NIF), are essential to assuring safety, reliability, and effectiveness of the nuclear force; these capabilities are invaluable to the nation's Stockpile Stewardship Program (SSP). A significant information gap exists in the hydrodynamic response to nuclear detonations that occur near the earth's surface. Numerical simulation methods were used to evaluate the hydrodynamic response of earth-like materials and to develop the energy coupling/partitioning curve for low yield nuclear detonations close to the earth's surface. Using LLNL's supercomputers and GEODYN hydrodynamic code, the properties of stress, pressure, and energy were evaluated for twelve simulated 2.5kT detonations; six above the surface and six below the surface. The results indicate stronger air blasts for detonations above or near the surface and that energy coupling into the ground changes rapidly with detonation location over a very small range between the above-ground and below-ground interface. This work serves to provide a baseline model to evaluate stress, pressure, and energy in relation to nuclear yield close to the earth's surface. The results support a better understanding of the physics of near-surface detonations and also assist in planning future experimental work at NIF.

THIS PAGE INTENTIONALLY LEFT BLANK

TABLE OF CONTENTS

I. INTRODUCTION 1

II. PROBLEM SETUP 3
- A. DEFINING THE PROBLEM 3
- B. SCALING 3

III. PHYSICAL CONFIGURATION 7
- A. NIF CONFIGURATION 7
- B. CONFIGURATION OF NIF EXPERIMENTAL DESIGN AND CORRESPONDING GEODYN SIMULATIONS 10
  - 1. Above Ground Configuration 11
  - 2. Below Ground GEODYN Configuration 13

IV. PHYSICS BEHIND THE CODE 17
- A. GEODYN BASICS 17
- B. THERMODYNAMICS 18
- C. CONTINUUM MECHANICS 19

V. METHOD 23

VI. ENERGY COUPLING 35

VII. CONCLUSION 49

APPENDIX A 51

APPENDIX B 63

LIST OF REFERENCES 73

INITIAL DISTRIBUTION LIST 75

THIS PAGE INTENTIONALLY LEFT BLANK

LIST OF FIGURES

Figure 1. Pressure Wave at Gauge #2 5
Figure 2. Target Chamber Interior w/ Diagnostic Instrument Manipulator 8
Figure 3. Target Chamber Exterior 8
Figure 4. Set Up Drawing 9
Figure 5. DIM and Chamber 10
Figure 6. Close Up View of the DIM 10
Figure 7. 3cm Height of Burst Calculation Set Up; Z-and R- axis in millimeters 12
Figure 8. 3cm Depth of Burial Calculation Set Up; Z-and R-axis in millimeters . 15
Figure 9. Pressure Wave at Air Gauge 1 for 1cm HOB 24
Figure 10. Pressure Wave at Air Gauge 2 for 1cm HOB 24
Figure 11. Pressure Wave at Ground Gauge 1 for 1cm HOB 25
Figure 12. Pressure Wave at Ground Gauge 2 for 1cm HOB 25
Figure 13. Pressure Wave at Ground Gauge 3 for 1cm HOB 26
Figure 14. Stress wave propagating through the Macor object 27
Figure 15. Tension waves propagating through the Macor object 27
Figure 16. Pressure Wave at Air Gauge 1 for 3cm DOB 28
Figure 17. Strange Pressure Wave at Air Gauge 2 for 3cm DOB 29
Figure 18. Strange Pressure Wave at Nominal Air Pressure Gauge 3 30
Figure 19. Modified Depth of Burial Set Up 31
Figure 20. Pressure at PG2 with Modified Set up (no noise from boundary) 31
Figure 21. Pressure profile for nominal pressure gauge 3 (PG3) 32
Figure 22. Pressure Wave at Ground Gauge 1 for 3cm DOB 32
Figure 23. Pressure Wave at Ground Gauge 2 for 3cm DOB 33
Figure 24. Pressure Wave at Ground Gauge 3 for 3cm DOB 33
Figure 25. Air blast is strongest for surface burst 35
Figure 26. Ground shock is the strongest for a buried burst 36
Figure 27. Energy in Macor block for several HOB shots 37
Figure 28. Energy in Macor block for several DOB shots 37
Figure 29. Split view of Material and Pressure at 35 microseconds for 10mm DOB shot 38
Figure 30. Split view of Material and Pressure at 120 microseconds for 20mm DOB shot 39
Figure 31. Split view of Material and Pressure at 120 microseconds for 30mm DOB shot 40
Figure 32. Corrected Plot of Energy in Macor block for several DOB shots 41
Figure 33. Lab Frame Energy Coupling Curve 41
Figure 34. World Frame Energy Coupling Curve 43
Figure 35. Energy Coupling Curve for Hard Rock 44
Figure 36. Matched Coupling Curve 45

THIS PAGE INTENTIONALLY LEFT BLANK

LIST OF TABLES

Table 1. Physical Properties of Macor glass ceramic 7
Table 2. Distances from target to pressure sensors 9
Table 3. MACOR and Limestone Comparison 11
Table 4. Constitutive Equations 18
Table 5. Scaled Depth of Burial 43
Table 6. Equivalent Yield Coupling Factor from simulation data 46
Table 7. Equivalent Yield Coupling Factor from live data fit curves 47

THIS PAGE INTENTIONALLY LEFT BLANK

LIST OF ACRONYMS AND ABBREVIATIONS

CTBT	Comprehensive Nuclear Test Ban Treaty
DIM	Diagnostic Instrument Manipulator
DOB	Depth of Burial
DOE	Department of Energy
ECYF	Energy Coupling Yield Factor
GPG1	Ground Pressure Gauge 1
GPG2	Ground Pressure Gauge 2
GPG3	Ground Pressure Gauge 3
HOB	Height of Burst
LLNL	Lawrence Livermore National Laboratory
MATLAB	Matrix Laboratory (software application)
NIF	National Ignition Facility
NNSA	National Nuclear Security Administration
PG1	Pressure Gauge 1
PG2	Pressure Gauge 2
PVDF	Polyvinylidine Fluoride
SBSS	Science Based Stockpile Stewardship
SSP	Stockpile Stewardship Program

THIS PAGE INTENTIONALLY LEFT BLANK

ACKNOWLEDGMENTS

I express my sincere thanks and appreciation to Dr. Craig Smith, Dr. Lew Glenn, and Dr. Benjamin Liu for their continued support and guidance given throughout this research. I gratefully acknowledge the many professors in the Physics Department at the Naval Postgraduate School for their dedication and attention.

I dedicate this work to my Pastor, and spiritual guide, Dr. Malachi K. York. Thank you for showing me Wu-Nuwaupu and for your guidance and mentorship, without which, I would not have had the motivation to persevere through this process.

THIS PAGE INTENTIONALLY LEFT BLANK

I. INTRODUCTION

From July 1945 to September 1992, the United States conducted 1,054 nuclear tests and executed two nuclear attacks. Considering the tests performed by other nuclear weapon states, the number of nuclear tests done by the U.S. nearly doubles that number. Since the initial scientific discovery of nuclear fission and the early development of nuclear weapon technology, the international situation has matured considerably, and there has been an increasing concern about the potentially harmful environmental and public health effects of nuclear testing, in addition to the devastating results of nuclear war. Over the decades, there have been many efforts on the part of the United States to reduce the threat of nuclear weapons. These efforts culminated in August of 1995 when, then President Bill Clinton, announced the Comprehensive Test Ban Treaty (CTBT), which would institute a worldwide ban on the testing of nuclear weapons of any yield. This treaty was signed by the United States in September 1996 at the United Nations, though the agreement has not yet been ratified by the U.S. Senate and, thus, has not officially entered into force. Nevertheless, the U.S. and other nations have complied with the major features of the treaty, and a de facto ban on nuclear weapons testing has emerged.

Given the current de facto ban on nuclear testing, in order to remain confident in the safety, reliability, security and deterrent effectiveness of the existing nuclear weapons arsenal, while retaining proficiency in nuclear technology, methods other than nuclear testing have been developed [1]. The Science-based Stockpile Stewardship (SBSS) Program was established to: increase the understanding of the current nuclear stockpile, predict and evaluate potential problems as these nuclear weapons age, fix or re-manufacture weapon components, and maintain proficiency and credibility to support the deterrent value of potential nuclear weapon use in the future [2]. According to the U.S. DOE/NNSA, “Computer models and advanced experimental capabilities that provide accurate predictive capability of weapon performance in the absence of

nuclear testing became the main goal of the National Nuclear Security Administration's Stockpile Stewardship Program."[2] The National Ignition Facility (NIF) at Lawrence Livermore National Laboratory serves as a vital tool to the nation's Stockpile Stewardship Program. NIF is currently the largest laser system ever built in the world. It has the capability to achieve pressure and temperature conditions that are replicated only in nuclear weapons, the sun, and stars, albeit on a much smaller scale [1].

During the era of nuclear weapons testing, there were many experiments conducted that measured the hydrodynamic properties and shock response of materials above and below ground. There is a wealth of knowledge documented from the nuclear tests that were conducted, but the majority of these nuclear tests took place either at altitudes well above ground level or at depths of burial well below the ground surface. Consequently, there is little data of the hydrodynamic response of materials to a nuclear detonation at or near the earth's surface. Given the current ban on nuclear testing, large-scale testing of weapons cannot fill such data gaps; however, LLNL's National Ignition Facility offers a unique capability to generate data in this region of interest that cannot be duplicated by any other conventional means. Employing the laser technology of NIF, along with advanced numerical computation methods, data can be produced that give insight to both the hydrodynamic response of materials, and the shock physics that takes place during and after a nuclear detonation at or near the earth's surface. The data generated will serve particular interests in the fields of nuclear detonation detection and verification, nuclear forensics, and structural survivability. The primary objective of this thesis research is to perform a series of simulation calculations to analyze and support the planning of NIF experiments designed to characterize the shock response of a prototypical material from near-surface detonations, and to generate an energy coupling plot that shows the air/ground energy coupling and the energy partitioning between air and ground that results from nuclear detonations occurring at or near the earth's surface.

II. PROBLEM SETUP

A. DEFINING THE PROBLEM

The principal factors that distinguish a nuclear detonation from conventional detonations are specific energy and yield. The two nuclear weapons used in the attacks conducted by the United States on Hiroshima and Nagasaki had yields of 12–15 kilotons of TNT equivalent and 20–22 kilotons of TNT equivalent, respectively. In a NIF experiment simulating an actual weapon detonation, the experimental setup must be planned to properly scale down the physical dimensions and characteristics of the event. In order to properly mimic the conditions of a low yield nuclear explosion, the parameters of energy, length, and time must be scaled down to the lab frame. The National Ignition Facility has 192 laser beams each with the capability of delivering approximately 9.4kJ of energy for a combined total of 1.8MJ of light energy. NIF can generate a peak power of 500 trillion watts, which is 1,000 times the electric generating power of the entire country [3]. High-precision lasers, such as these, allow for the achievement of specific energies that are near those of nuclear devices. This opens up a window of opportunity to investigate the physics of near-surface nuclear detonations. For the experiments being considered, only four of the 192 laser beams will be used, with each contributing only 2.5kJ (i.e., operating at roughly 25% capacity), to achieve a total deposited energy of 10kJ focused into a 2mg cylindrical hohlraum,[1] which yields a specific energy of 5MJ/g. This cylindrical hohlraum has a height and diameter of about 2mm and a volume 100 times smaller than that of a pencil eraser.

B. SCALING

To scale the experiment down to the laboratory frame, the Glasstone/ Dolan cube root scaling law was used:

[1] A small gold cylinder named after the German word for “hollow room” that serves as the target for a NIF experiment.

> Theoretically, a given pressure will occur at a distance from an explosion that is proportional to the cube root of the energy yield. Full-scale tests have shown this relationship between distance and energy yield to hold for yields up to (and including) the megaton range. [4]

For the anticipated experiment relating a 2.5kT full-scale test to a NIF energy deposition of 10kJ, a scaling factor of 1000 can be derived as follows:

$$(2.5kT/10kJ)^{1/3} = [2.5kT*(4.184x10^{9}kJ/kT)/10kJ)]^{(1/3)} \sim 1000$$

$$\text{where } 1kT = 4.184*10^{12}J$$

To elaborate, in an actual 2.5 kT yield detonation, the energy release is:

2.5kT = 10.46 x 10^{12} J = 10.46 x 10^{9} kJ

This experimental NIF energy deposition of 10kJ in comparison with the detonation release of 2.5kT represents an energy reduction factor of:

(2.5kT/10kJ) = (10.46 x 10^{9} kJ/10 kJ) ~ 10^{9}

Applying Glasstone and Dolan's cube root scaling factor rule, the resulting scaling factor is 10^{3}, or a factor of 1000 [4]. Another way to characterize the cube root scaling factor rule as applied to distance scaling is to recognize that:

$D_a = D_r * (W_a / W_r)^{1/3}$

where:

D_a=actual distance

D_r=reference distance

W_a=actual yield

W_r=reference yield

Therefore, in the case being considered where the energy reduction factor is 10^{9}, the distance scaling is a factor of one thousand. A similar calculation is also applied to the time parameter. As a result, with both time and distance properly scaled, the physical properties such as particle velocity, pressure, density, and temperature are accurately reflected without scale factors. The

primary properties of interest in this thesis are those of pressure and energy, which will be used to construct the energy-coupling curve as the height of burst/ depth of burial is varied for a 2.5kT simulated explosion.

For example, Figure 1 presents the results of a simulation of a 10kJ NIF experimental explosion at a height of burst of 3cm (corresponding to a 2.5kT nuclear detonation at a height of burst of 30m), in which the pressure wave reaching a maximum of .8MPa (8 bar), arrives in approximately 80 microseconds at a sensor location (Gauge #2) 15 cm from the explosion. This would scale back to the real world reference frame as a shock with the same peak pressure of 8 bar arriving in approximately 80 milliseconds at a distance of 150 meters away from an explosion of 2.5kT yield at a height of burst of 30 meters.

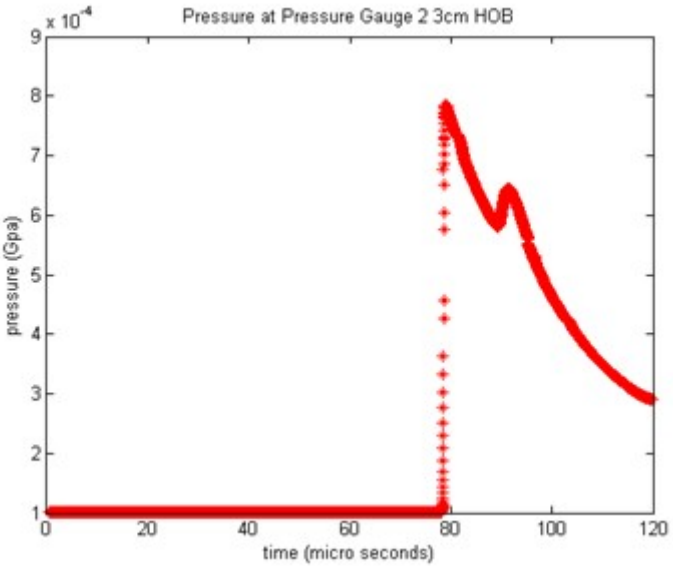

Figure 1. Pressure Wave at Gauge #2

THIS PAGE INTENTIONALLY LEFT BLANK

III. PHYSICAL CONFIGURATION

A. NIF CONFIGURATION

For a series of anticipated NIF experiments to investigate near-surface detonation coupling, four of the 192 laser beams will be used. Each beam contributes 2.5 kJ of energy over two nanoseconds that will be deposited in a 2mg cylindrical hohlraum. The four lasers will combine inside the near-vacuum target chamber, as shown in Figures 2 and 3, and focus directly into the gold hohlraum target. The gold will essentially vaporize and expand as a gold gas pill. This is similar to physical conditions in the detonation of a full scale nuclear device where all components are vaporized and contribute to the ensuing fireball. The gold hohlraum will be located 30mm above the surface of a cylindrical core of a ceramic material called Macor[2], which for the purpose of these experiments, simulates the solid material of the earth's surface. The properties of the Macor ceramic, some of which are listed Table 1, are similar to the properties of many solid earth materials, in particular limestone. The Macor ceramic in the experiment serves as a model for the ground response to a nuclear detonation over limestone.

Density	2520 kg/m^3
Young's Modulus	64.1 GPa
Shear Modulus	25.4 GPa
Poisson's Ratio	0.26
Quasi-static compressive strength	345 MPa

Table 1. Physical Properties of Macor glass ceramic (From W.Chen, 1997, p.1310)

[2] Macor is a machinable white glass ceramic.

Figure 2. Target Chamber Interior w/ Diagnostic Instrument Manipulator

Figure 3. Target Chamber Exterior

The experimental target consists of a hohlraum target (representing the scaled down nuclear device) and the pre-fabricated Macor cylinder which will include three pressure sensors embedded into the structure in addition to the hohlraum, and two additional pressure sensors mounted outside of the Macor object in order to measure pressure in the region representing the near-surface atmosphere. From the focal point of the laser beam, the pressure gauges[3] will be located at the straight-line distances shown in Table 2.

[3] PG1 and PG2 represent the two atmospheric pressure sensors external to the Macor object while GPG1 through 3 represent the pressure sensors embedded within the Macor object.

Pressure Gauge 1 (PG1)	10cm
PG2	15cm
Ground Pressure Gauge 1 (GPG1)	5cm
GPG2	7cm
GPG3	10cm

Table 2. Distances from target to pressure sensors

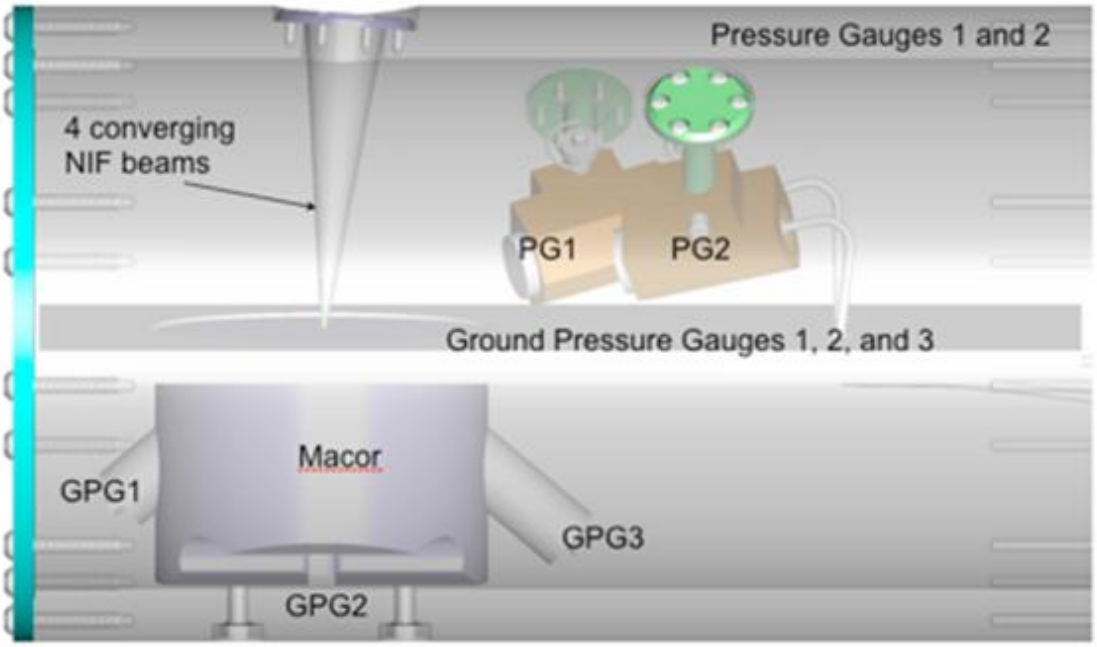

Figure 4. Set Up Drawing After [6]

Figure 4 shows a diagram of the experiment, self contained in a cylindrical casing that will be inserted on the diagnostic instrument manipulator (DIM) depicted in Figure 5. The subsurface sensor, GPG2, has a quartz piezoelectric element with a dynamic range of 0-2 GPa and a bandwidth of 1-100 MHz. The subsurface sensors GPG1 and GPG3, located at 45-degree angles from the laser vector in its focal point, have polyvinylidine fluoride (PVDF) piezoelectric elements, which provide longer recording times, and each has a dynamic range of 0-2 GPa and a bandwidth of 1-100 MHz. PVDF is a piezoelectric plastic polymer that is commonly used as a shock sensor [7]. The above-surface sensors PG1 and PG2 have PVDF elements and have a dynamic range of 0-6

MPa and a bandwidth of 30kHz to 3MHz. The Macor cylinder will be inserted into the NIF target chamber attached to the diagnostic instrument manipulator (DIM), shown in Figures 5 and 6.

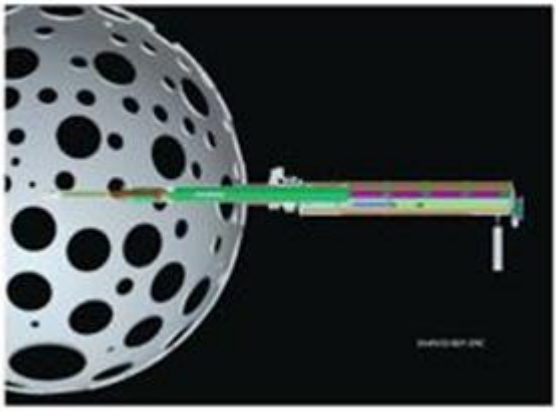

Figure 5. DIM and Chamber

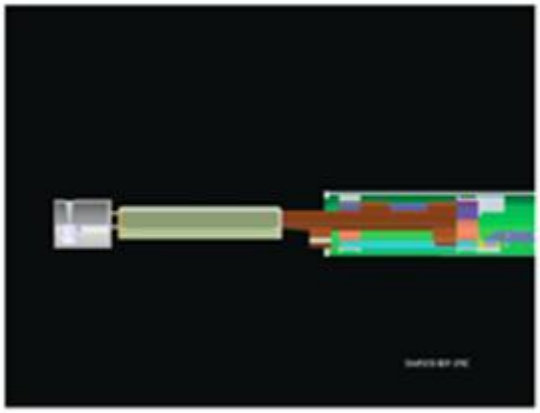

Figure 6. Close Up View of the DIM

B. CONFIGURATION OF NIF EXPERIMENTAL DESIGN AND CORRESPONDING GEODYN SIMULATIONS

In order to properly model the experiment simulating a nuclear detonation over or in limestone, a combination of materials with similar properties to that of limestone and air must be used. With Macor as the solid material, the gas mix was selected by empirical methods to mimic as close as possible atmospheric

density. The required gas mix was calculated to consist of 65% Ne, 20% Ar, 10% Kr, and 5% Xe. This mixture yields similar results in terms of transmission and absorption of the soft x-rays emitted in order to produce a scaled deposition of the x-rays and the "double peak" intensity plot that is characteristic of nuclear detonations. The first peak in light intensity is due to the initial reaction and expansion of hot gas in the form of a fireball. Quickly, the shock wave from the explosion expands past the fireball and the air outside the fireball is compressed by the shock wave to the point of becoming opaque to light. As the shock wave expands spherically, the pressure front decreases and the light from the fireball is once again visible [8]. Table 3 presents a summary comparison of the properties of the Macor/artificial atmosphere, and limestone/normal atmosphere which demonstrates their similarities.

PROPERTY	GAS MIX OVER MACOR	AIR OVER LIMESTONE
'Atmospheric' density	.00153 g/cc	.001204 g/cc
'Ground' density	2.52 g/cc	2.59 g/cc
'Ground' sound speed	4.58 km/s	3.67 km/s

Table 3. MACOR and Limestone Comparison After [6]

To achieve the objective of this thesis, a series of simulations using LLNL's GEODYN[4] computer code was carried out to analyze the experimental configuration for planning purposes and also to develop response projections to establish the ground-coupling curve. The first set of simulations were carried out to represent the hydrodynamic response to detonations (and NIF experiments representing) above-ground detonations. The second set treated below-ground detonations.

1. Above Ground Configuration

Figure 7 presents an experimental plan and the corresponding simulation layout for the above-ground case.

[4] More information about GEODYN can be found at https://e-reports-ext.llnl.gov/pdf/326532.pdf.

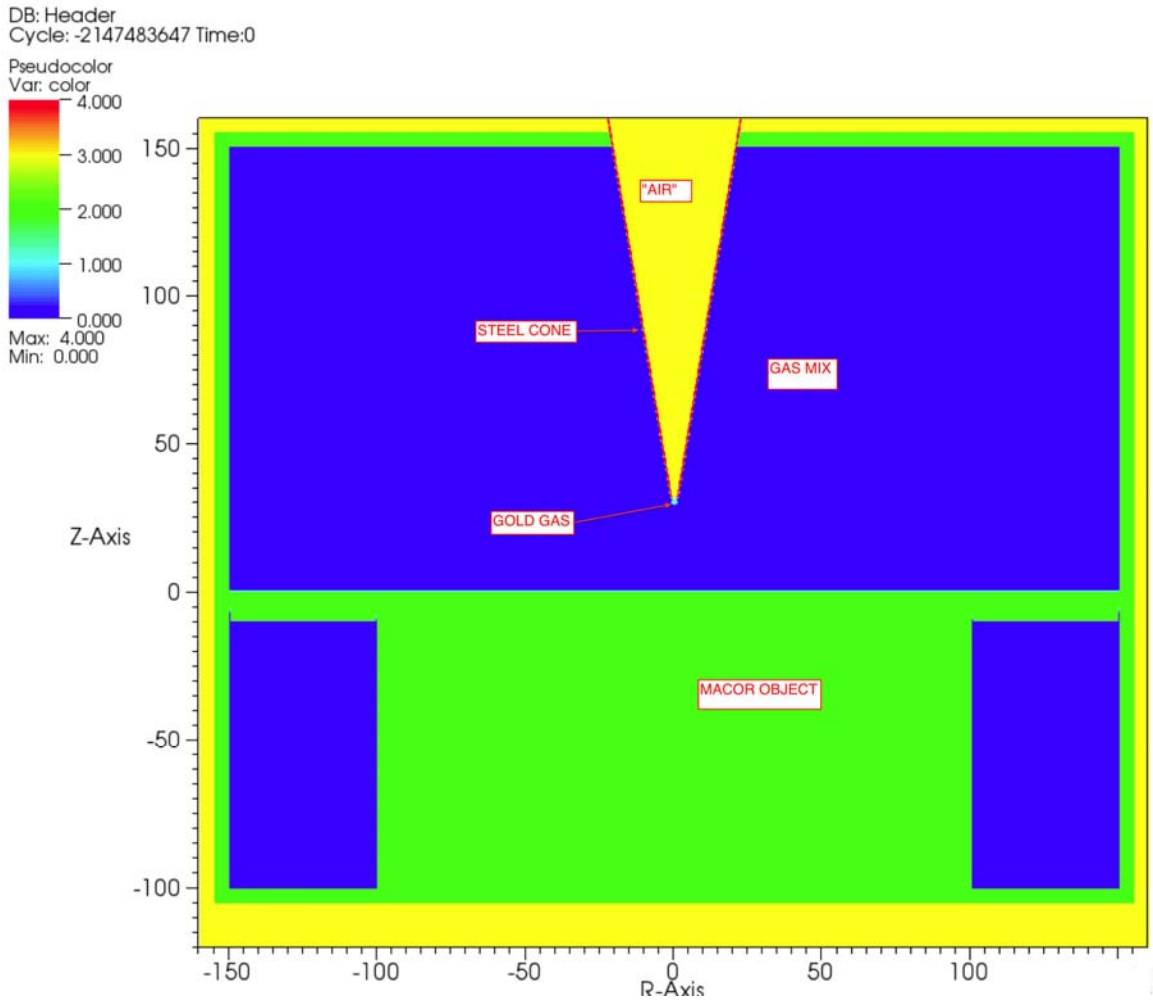

Figure 7. 3cm Height of Burst Calculation Set Up; Z-and R- axis in millimeters

In this portion of the simulations, a simplified 2D axisymmetric geometrical representation of the physical configuration was constructed. Figure 7 shows the output of LLNL's graphics software, VisIT[5], at time zero, as the initial set up in the GEODYN computer modeling code. In the above-ground model setup, there are five materials—Macor, the atmospheric gas-mix, gold, "air,"[6] and steel. The purposes of the first three materials are obvious, but the latter two require

[5] VisIT is an interactive parallel visualization and graphical analysis tool for scientific data capable of handling data on the terabyte scale.

[6] The "air" is given an extremely low density to simulate the vacuum conditions, through which the lasers propagate, inside the NIF target chamber.

additional explanation. Within the computer model, there must be a replication of the vacuum barrier through which the lasers propagate to deposit the energy inside of the gas mix for an above-ground calculation. In this simulation, a hollow steel cone is used to represent the vacuum barrier and to keep that vacuum separate from the gas mix. (See Appendix A) Essentially, the simulation begins after all the energy from the laser is deposited into the gold hohlraum. This was achieved by creating a steel cone with an apex at the laser focal point. In the simulation, the steel cone is filled with "air," but given a density of almost zero, so that it does not contribute to the forming shock wave. The actual pressure anticipated inside of the NIF target chamber is close to 10^{-5} millitorr at the time of a target shot. By changing the location of the apex of the steel cone (and the attached hohlraum target), the desired height of burst for the calculation is achieved. In order to record the changes in the hydrodynamic properties as the experiment evolves, marker files were embedded throughout the configuration with the primary markers being geometrically located at the same places that the subsurface and aboveground pressure sensors are located. Each of the five materials is indexed for identification with label values from 0 to 4 and given a density and a strength parameter and defined by a series of coordinate points. The input file for the 10mm height of burst simulation can be found in Appendix A for further clarification.

2. Below Ground GEODYN Configuration

The depth of burial simulation set up is similar to that of the height of burst simulations, with the exception that there is no need to incorporate the steel cone, as the energy is deposited directly into a hohlraum embedded in the Macor block. Figure 8 shows the initial set up of the simulation, in VisIT, for the below-ground case. The subsurface calculations are done from an idealized point of view. The Macor is uniformly manufactured and the Macor representation is uniform. This is a limitation in terms of representing real-world earthen structures, which are far from uniform. The possible addition of cracks, porosity, or other heterogeneities within the simulated Macor is not addressed in this work

but may be a topic for future study. Additionally, in terms of mimicking a setup for a NIF experiment there must be a conduit through which the energy, from the laser, is deposited. Essentially this would involve constructing an inverted hollow cone with an apex beneath the surface. The amount of energy that remains in the region of the cone as opposed to being contained completely in the “ground” must also be taken into consideration when calculating the energy coupling. It must be stressed that the depth of burial simulations conducted in this work were done from an ideal standpoint. This would be the real world equivalent of digging a cavity into the ground, placing a 10kJ nuclear device in the cavity, and then covering the cavity and packing it to the ground’s original density. These depths of burial calculations serve as a baseline used to construct the energy coupling curve.

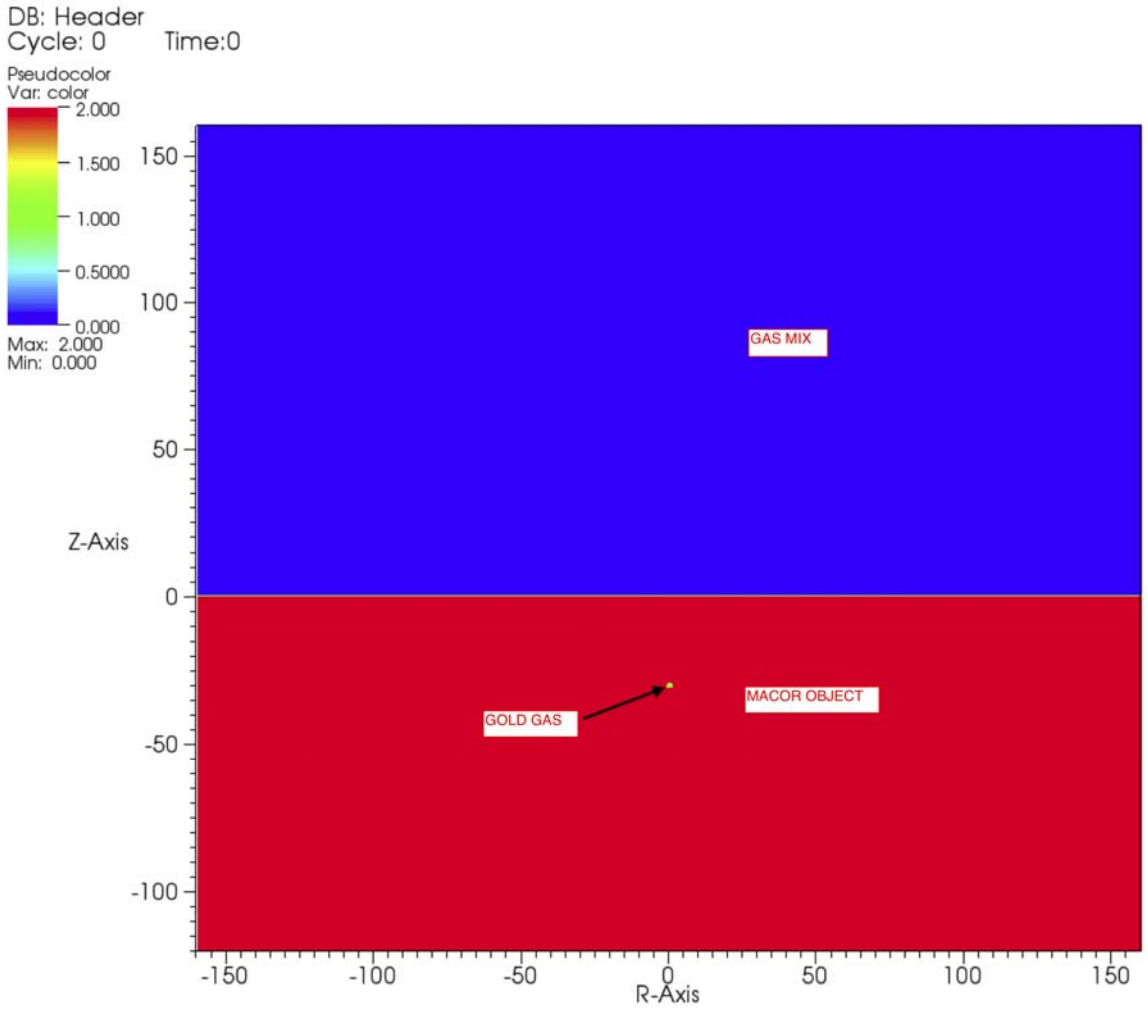

Figure 8. 3cm Depth of Burial Calculation Set Up; Z-and R-axis in millimeters

THIS PAGE INTENTIONALLY LEFT BLANK

IV. PHYSICS BEHIND THE CODE

A. GEODYN BASICS

In order for a hydrodynamic simulation to have validity, it must be constrained so as to obey the laws of physics. The hydrodynamic code used in this thesis, called GEODYN, was developed at LLNL and incorporates physical models to fully describe a broad range of phenomena including shock and thermodynamic behavior. It is an Eulerian code with adaptive mesh refinement (AMR). There are two basic types of dynamic codes, Lagrangian and Eulerian. A Lagrangian code's mesh, or background, moves with the material, so no mass flows between cells. In an Eulerian code, the mesh or background is stationary and the material is allowed to move though stationary cells. An Eulerian code is analogous to looking at a dust storm through a window whereas a Lagrangian code is analogous to floating along with an individual dust particle in the storm. The adaptive mesh means that the code has the ability to vary the level of detail of the background. In keeping with the dust storm analogy, the adaptive mesh is analogous to having the ability to simultaneously have small microscopic windows to capture the details of small grains and larger windows for use when detail is not needed. An Eulerian code with adaptive mesh refinement such as GEODYN allows for rigorous high numerical resolution in areas in one part of a problem and less refined, less sensitive areas in another.

When dealing with shock physics, high temperatures, and nuclear interactions, the laws of physics that constrain the results are numerous. The two primary areas of physics that are of concern are thermodynamics and continuum mechanics. The GEODYN code simplifies the matter without deviation from real experimental results by implementing the various physics constraints into a formulation based on both the 1st and 2nd laws of thermodynamics, and the laws of conservation of mass, momentum and energy [9].

GEODYN is a complex modeling code. In order to provide some background information on key physics processes taking place in GEODYN, the remaining sections in this chapter, (Sections B and C), provide some mathematical derivations of some of the physics involved in terms of thermodynamics and continuum mechanics respectively.

B. THERMODYNAMICS

A major portion of GEODYN, summarized in Table 4, are the constitutive equations that express specific entropy, specific internal energy, stress, and heat flux in terms of: temperature (θ), change in temperature ($\Delta\theta$), deformation gradient (F) and the change in deformation gradient (dF).

Specific entropy (s)	$s=s(\theta,\Delta\theta,F,dF)$
Specific internal energy (u)	$u=u(\theta,\Delta\theta,F,dF)$
Stress (T)	$T=T(\theta,\Delta\theta,F,dF)$
Heat flux (q)	$q=q(\theta,\Delta\theta,F,dF)$

Table 4. Constitutive Equations

These constitutive equations can be derived from the Clausius-Duhem inequality[7], which has been derived below for clarification.

Consider the following five parameters of interest:

1. Specific entropy s
2. Mass density of the body ρ
3. Internal heat supply/ (mass-time) r
4. Outward heat flux vector q
5. Temperature θ

[7] The Clausius-Duhem inequality is used in continuum mechanics to express the second law of thermodynamics.

The entropy (due to heat transfer into a system) is given by the following formula[8]:

$$\frac{ds}{dt} = \int_{Volume} \rho r / \theta dv + \int_{Surface} -q / \theta da$$

where dv and da represent the defferentials of volume and area respectively.

However, when dealing with real, irreversible processes the thermodynamic equations become inequalities. So, the change, with respect to time of the entropy, would be

$$\frac{d}{dt} \int_{Volume} s\rho dv \geq \int_{Volume} r\rho / \theta dv + \int_{Surface} -q / \theta da .$$

Using the divergence theorem (integral over area is equal to the integral of the divergence over a volume), the expression becomes:

$$\frac{d}{dt} \int_{Volume} s\rho dv \geq \int_{Volume} r\rho / \theta dv - \int_{Volume} \nabla \bullet (q / \theta) dv .$$

This is the integral form of the Clausius-Duhem inequality. The Clausius-Duhem inequality in its most recognized form is in the differential form:

$$\frac{ds}{dt} \geq r / \theta - 1 / \rho * \nabla \bullet (q / \theta).$$

This formula states that the rate of entropy change, with respect to time, in a system is greater than the rate of entropy change due to heat transfer into the system.

C. CONTINUUM MECHANICS

The next major portion of GEODYN deals with how a material deforms, or flows over time, due to energy input; all while conserving mass, energy, and

[8] The mathematical derivations that follow are summaries based upon detailed presentations in [9].

momentum. The equations used are often in the form of the convective derivative (deformation/ flow equation); for example

$$\frac{D}{Dt}(\#) = \frac{\delta}{\delta t}(\#) + V \bullet \nabla(\#).$$

This equation states that the total change, with respect to time, is equal to the change in the fixed frame, plus the change in the moving frame. In effect, this is a continuity equation. The parameter denoted by the # sign represents a history-dependant scalar parameter such as porosity, temperature, or plastic strain and V (capitalized) represents the velocity of the fluid medium. The derivation of the generic continuity equation is shown below for the purpose of providing clarification for what is taking place mathematically in the GEODYN code.

Let L be some intensive (mass independent) property defined over a control volume Ω. The parameter Q represents sources and sinks in the fluid. The rate of change of L is given by the formula below:

$$\frac{d}{dt}\int_{\Omega} L dv = -\oint_{Surface} LVnda - \int_{\Omega} Q dv$$

where dv and da represent the defferentials of volume and area respectively

Applying the divergence theorem to the 1st term on the right side of the equal sign gives:

$$\frac{d}{dt}\int_{\Omega} L dv = -\int_{\Omega} \nabla \bullet (LV) dv - \int_{\Omega} Q dv$$

Combining the terms on side of the equation gives:

$$\int_{\Omega} (\frac{\delta L}{\delta t} + \nabla \bullet (LV) + Q) dv = 0$$

The above condition must be true for all dv; therefore, the following generic continuity equation results:

$$\frac{\delta L}{\delta t} + \nabla \bullet (LV) + Q = 0$$

This equation states that the amount of a conserved quantity, inside a defined region, can only change by the amount that passes through the boundary of the region in addition to any internal sources or sinks. The conservation of mass, energy, and momentum all follow from the above generic continuity equation.

In GEODYN, solid is modeled as an extension of a fluid, with the added appropriate strength parameters. A LLNL Mie-Gruneisen equation of state[9] was used to calculate the pressure in the Macor for this simulation. For the gold source, a tabular equation of state provided by LLNL was used.

[9] The Mie-Gruneisen equation of state is often used to measure the pressures in shock compressed solids.

THIS PAGE INTENTIONALLY LEFT BLANK

V. METHOD

A series of simulation calculations were performed in which the height of burst and depth of burial ranged from 5mm to 50mm. A simulation was run at 5mm, 10mm, 20mm, 30mm, 40mm, and 50mm for both above-ground and below-ground cases for a total of 12 simulations. On average, each simulation required a total 24 hours of computation, broken into three 8-hour periods on LLNL supercomputers. Each computation was considered complete once the shock front passed the location of the most distant shock sensor, which on average tended to be about 100 microseconds (real time), or about 24 hours of computation time. To achieve 12 complete data sets ranging from a depth of burial of 5cm to a height of burst of 5cm required a time period of three months. After each successful calculation, the data were analyzed using both MATLAB[10] and LLNL's visualization software VisIT[11]. GEODYN has the ability to track various parameters during the experiment. The parameters of interest are: pressure, density, material type, particle velocity in the r and z coordinate directions, sound speed, internal energy, total energy, and temperature. As stated earlier, in order to construct data showing the energy coupling between ground burst and air shock, the primary parameters of interest are pressure, particle velocity, time and total energy. Figures 9 through 13 present the pressure wave results for the 10mm height of burst calculation at the five sensor positions.

[10] MATLAB is a scientific software application used for matrix manipulation and plotting that can interface with other programming languages such as C, C++, and FORTRAN. See http://www.mathworks.com/products/matlab/.

[11] FOR ADDITIONAL DESCRIPTION OF VISIT, See https://wci.llnl.gov/codes/visit/about.html.

Height of Burst Plots

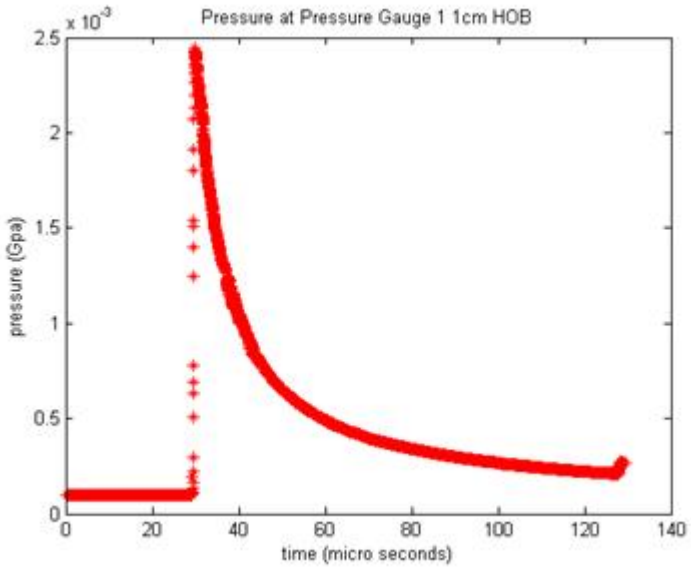

Figure 9. Pressure Wave at Air Gauge 1 for 1cm HOB

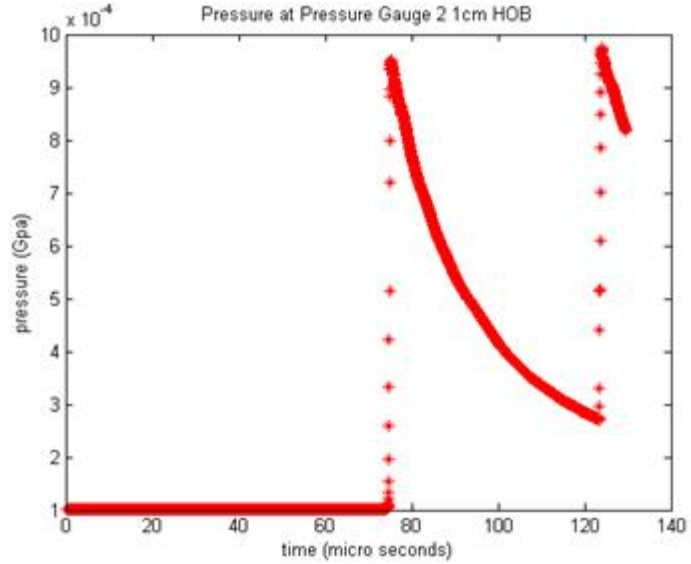

Figure 10. Pressure Wave at Air Gauge 2 for 1cm HOB

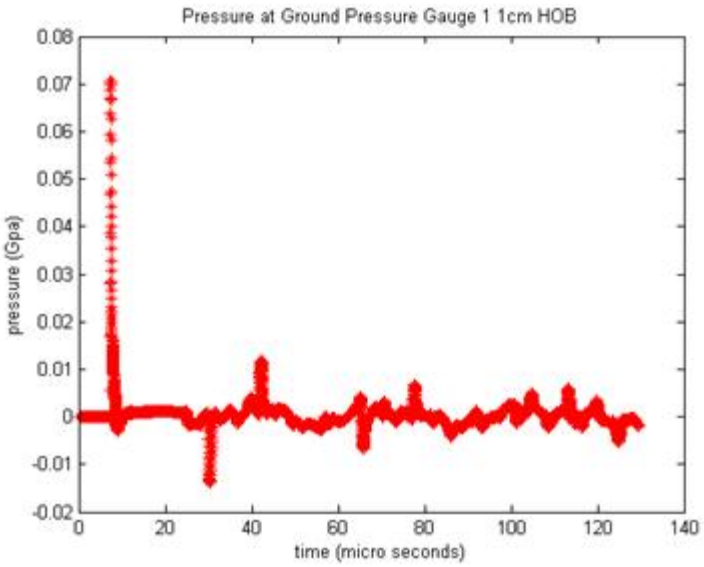

Figure 11. Pressure Wave at Ground Gauge 1 for 1cm HOB

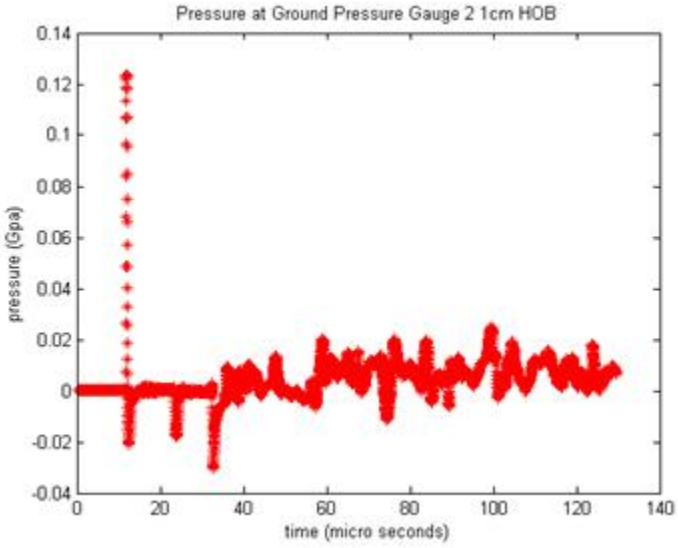

Figure 12. Pressure Wave at Ground Gauge 2 for 1cm HOB

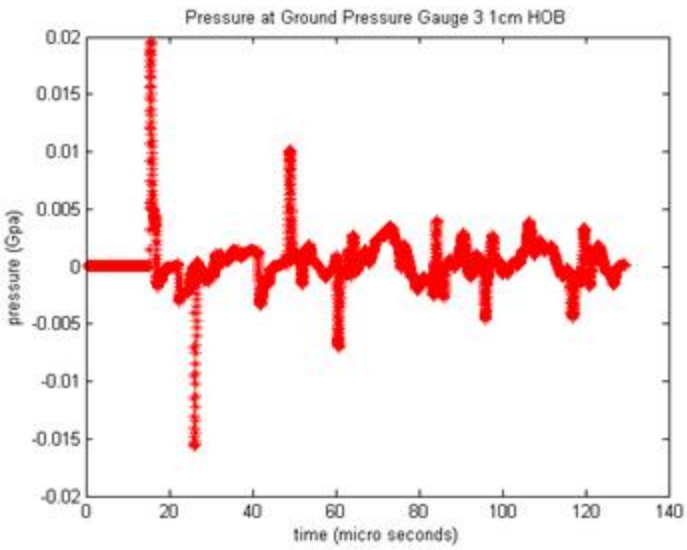

Figure 13. Pressure Wave at Ground Gauge 3 for 1cm HOB

The most useful information gathered from these plots is the peak pressure and the time of arrival of the peak pressure wave. This information served as a check for the calibration of the PVDF shock sensors. For Figures 10 through 13, after the initial pressure waves any other peaks are the results of boundary reflections. In the case of Figure 10 for PG2 a second pressure peak is visible at 120 microseconds. This second peak is due to the reflection of the initial blast wave from the Macor/gas-mix boundary. For Figures 11 though 13 the many reflection stress waves are the result of free surface reflections from the Macor/gas-mix boundary. Some of the interesting phenomena shown in the plots above were made clear when the data were analyzed using LLNL's visualization software, VisIT. For example, in the ground sensors, the stress waves in tension were easily identified by stepping through the calculation frame-by-frame in time. In the simulation, the Macor is surrounded by a free surface and thus tension waves occur at the intersection between the Macor block and the gas mix. Figure 14 shows a movie frame of the detonation at 11 microseconds, with pressure on the left and material on the right, where the initial stress wave propagating through the Macor object is visible. Figure 15 shows a

movie frame, at 24 microseconds, where the stress waves have reached the edges of the Macor object and reflected tension waves are clearly visible.

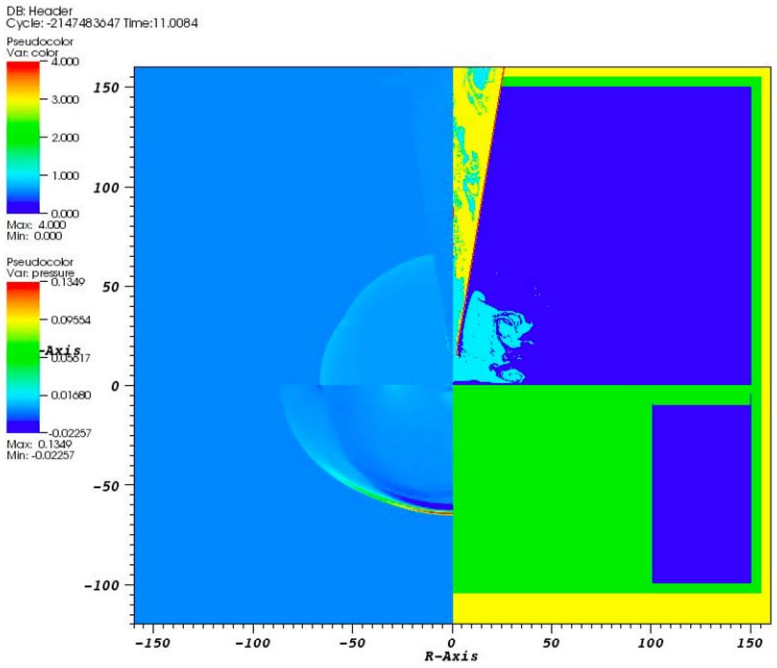

Figure 14. Stress wave propagating through the Macor object

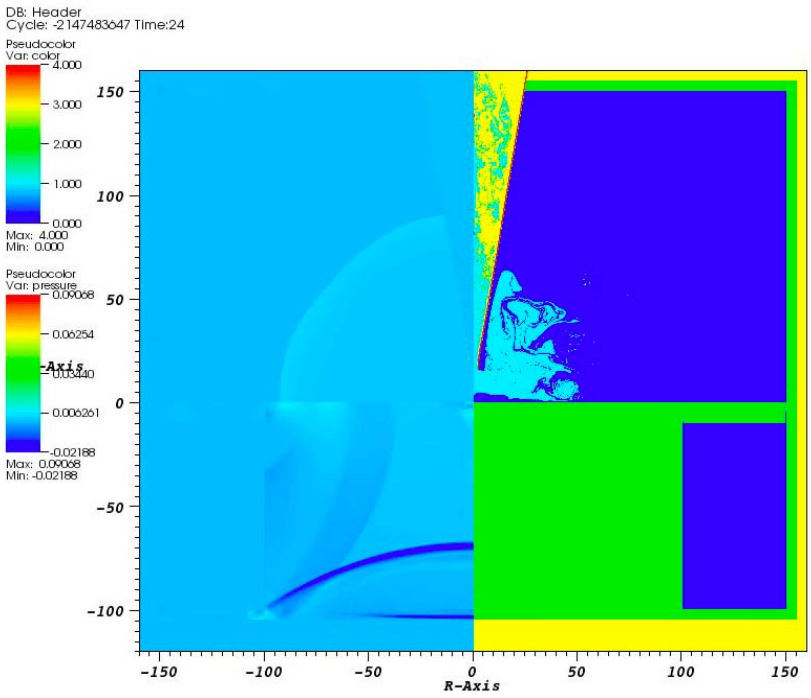

Figure 15. Tension waves propagating through the Macor object

Since, in the actual experiment, the Macor test object will be held on the DIM, the real fluctuation in pressure can be expected to be substantially less. The recovery period of the pressure sensor will also eliminate much of the reflected response, as the sensors will not be able to record continuously as in the simulation.

Depth of Burial Plots

The pressure waves for the five shock sensors, for a 30mm depth of burial simulation, are shown in Figures 16 through 20. Figure 16 shows that there was no air shock wave measured by PG1 for the 30mm depth of burial simulation. Figure 17 shows a strange wave profile in the shape of a ramp wave, indicative of a supported shock, (which should not be the case here as the 10kJ is deposited into the gold hohlraum within a few nanoseconds), for the air pressure gauge (PG2).

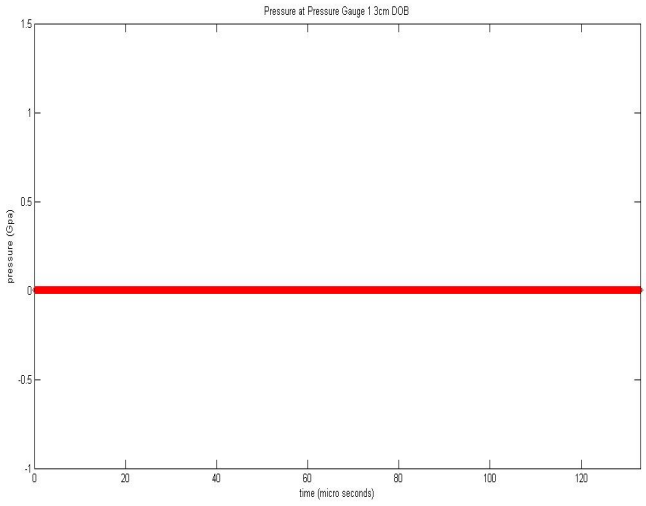

Figure 16. Pressure Wave at Air Gauge 1 for 3cm DOB

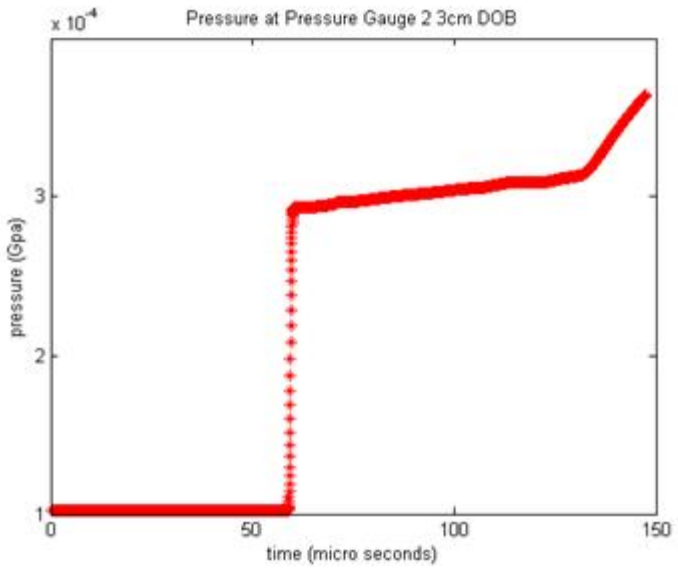

Figure 17. Strange Pressure Wave at Air Gauge 2 for 3cm DOB

Upon initial review of the data, it was unclear how the pressure profile in Figure 17 translated to what was happening mathematically in the simulation. The wave profile appears to indicate a pressure wave reflection that came from the boundary. To verify that this was indeed the case, further calculation was conducted in which an additional air sensor (PG3) was set up with an r-z coordinate of [25,140], which is closer to the boundary of the setup, to see if the pressure peak time of arrival was shorter than that in PG2. The results, shown in Figure 18, indicate the same anomaly in the pressure wave at the nominal 3rd air pressure gauge (PG3). The peak pressure time of arrival for the nominal PG3 sensor, arriving at approximately 40 microseconds, was shorter than the same anomalous wave in Figure 17 for PG2. This shows that the data is consistent with a wave that reflected from the boundary.

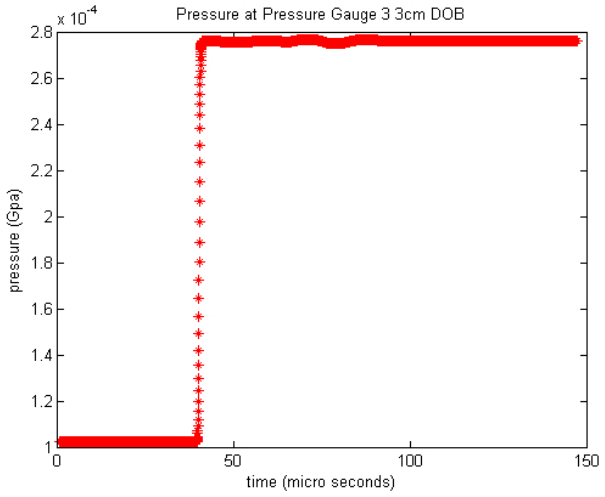

Figure 18. Strange Pressure Wave at Nominal Air Pressure Gauge 3

In order to eliminate the reflected wave noise from the depth of burial calculations the set up of the problem had to be modified. The boundary conditions of the problem are set up so that the system conserves energy, mass, etc. This issue did not arise in the height of burst calculation because there is a single material, "air," at the boundary. The issue arose in the depth of burial calculations because the boundary has two different materials, both Macor and gas-mix. To correct the setup, a thin layer of gas-mix was added around the Macor object in the input file and the simulations were run again (See Appendix B). Figure 19 shows the modified depth of burial setup. When performing the pressure analysis on the modified depth of burial calculations, the noise in PG2 vanished. Additionally the peak pressures in the three "ground" sensors in the Macor object were identical, which shows that the modification of the setup did not adversely affect the peak pressure readings. Figures 20 and 21 show the pressure wave profiles for PG2 and nominal PG3, which show that little to no shock was transmitted from the ground to the gas-mix (the pressure signal is down an entire order of magnitude from that in Figures 17 and 18), as expected.

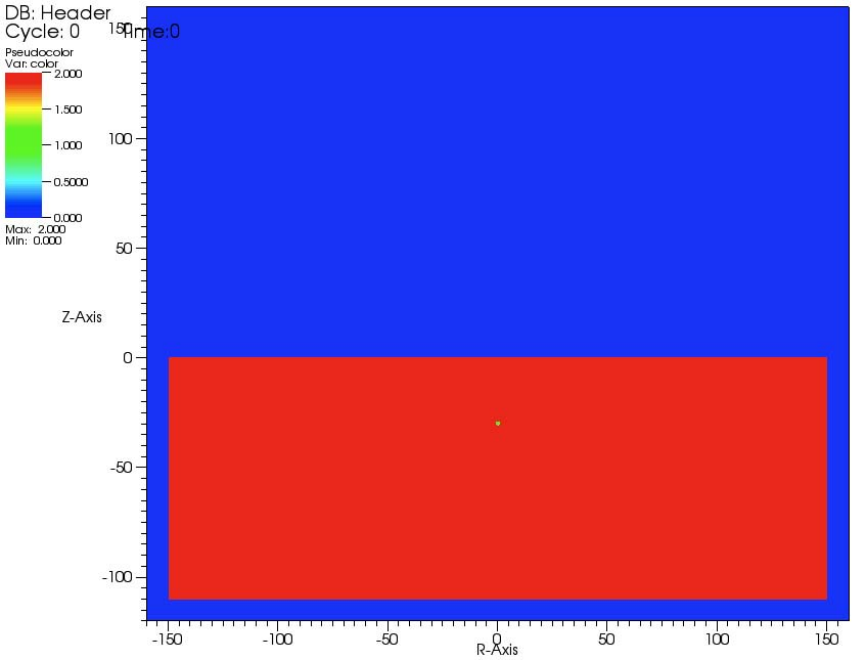

Figure 19. Modified Depth of Burial Set Up

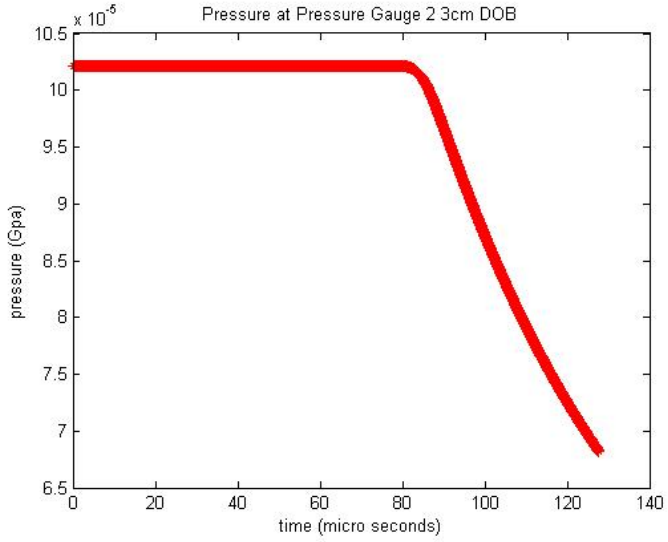

Figure 20. Pressure at PG2 with Modified Set up (no noise from boundary)

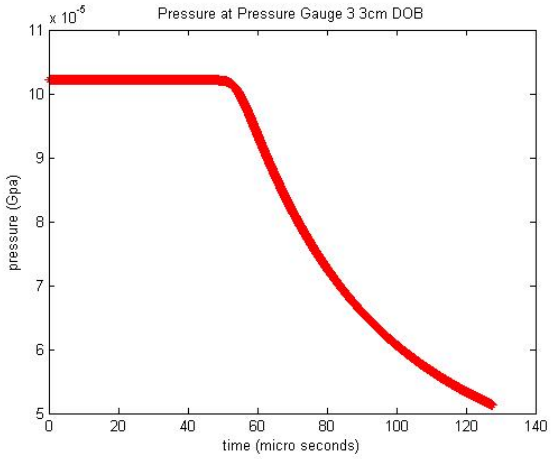

Figure 21. Pressure profile for nominal pressure gauge 3 (PG3)

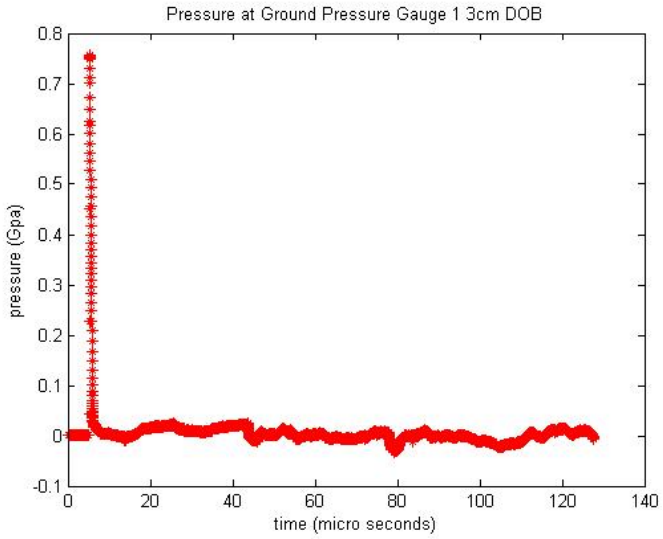

Figure 22. Pressure Wave at Ground Gauge 1 for 3cm DOB

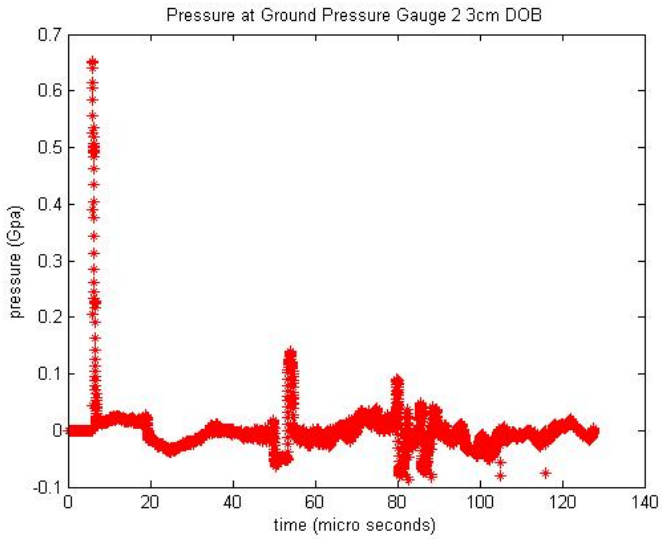

Figure 23. Pressure Wave at Ground Gauge 2 for 3cm DOB

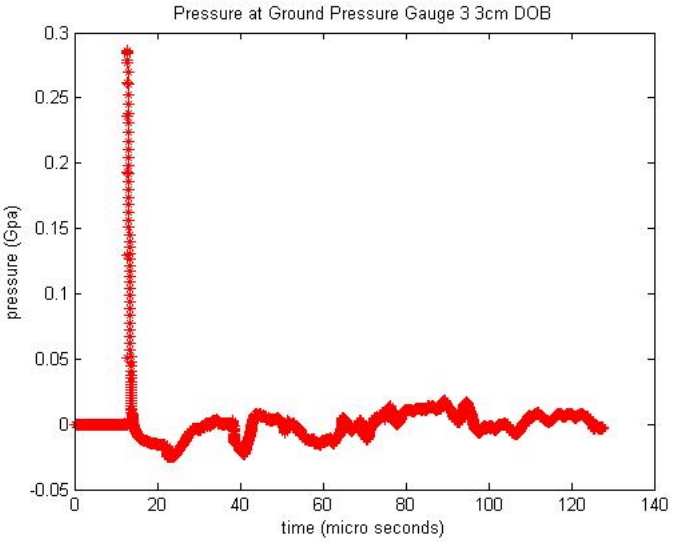

Figure 24. Pressure Wave at Ground Gauge 3 for 3cm DOB

As one would intuitively guess, the peak pressures calculated in the Macor object are much higher for the depth of burial shots. Again for Figures 22 through 24, the many reflection stress waves are the result of free surface reflections from the Macor/gas-mix boundary.

THIS PAGE INTENTIONALLY LEFT BLANK

VI. ENERGY COUPLING

In order to illustrate energy coupling and partitioning, two methods were used. The first method demonstrates the coupling by looking at the peak pressures for two pressure sensors for varied heights of burst and depths of burial. Figure 25 shows three pressure plots for three different heights of burst/ depth of burial from air pressure gauge 1 (PG1) superimposed on one another. Figure 26 shows three stress plots for three different heights of burst/ depth of burial from a ground sensor, (GPG3), superimposed on one another. These two sensors, PG1 and GPG3, were chosen because both are located at a distance of 10cm from the point of detonation. The r-z coordinates for PG1 are (8.6cm, 5cm) and the r-z coordinates for GPG3 are (7.07cm, 7.07cm) both yielding a range of 10cm. The three pressure curves correspond to two heights of burst and one depth of burial. The plot in Figure 25 shows that the air blast is strongest for detonations that occur near the surface. This may seem counterintuitive. The reason that the surface burst yields a stronger air blast is that the ground reflects much of the pressure wave, and the shock sensors detect the combined pressure of both the initial and the reflected shock.

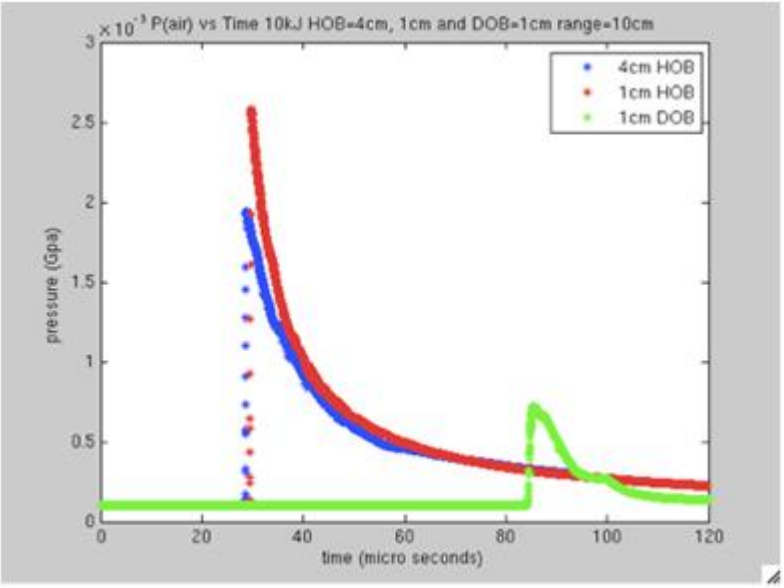

Figure 25. Air blast is strongest for surface burst

As reasonably expected, the results of the ground pressure/stress plots show that the ground shock is strongest for a buried burst.

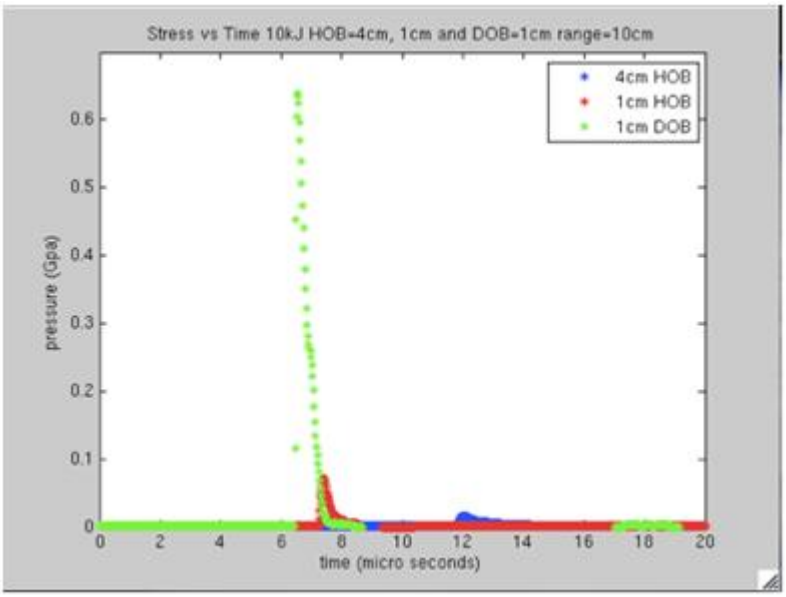

Figure 26. Ground shock is the strongest for a buried burst

The second method used to illustrate energy coupling and partitioning was to calculate the equivalent yield-coupling factor. This was done by plotting the total energy in the Macor block as a function of time for each height of burst and depth of burial calculation. The total energy transmitted into the Macor block for the height of burst simulations is straightforward. The total energy in the Macor varies inversely with the height of burst. At the theoretical limit of an infinite height of burst, there would be no energy transferred into the Macor block, and the only energy in the Macor would be due to its inherent mass energy. Figure 27 shows the energy transmitted into the Macor block as a function of time for each of the height of burst calculations.

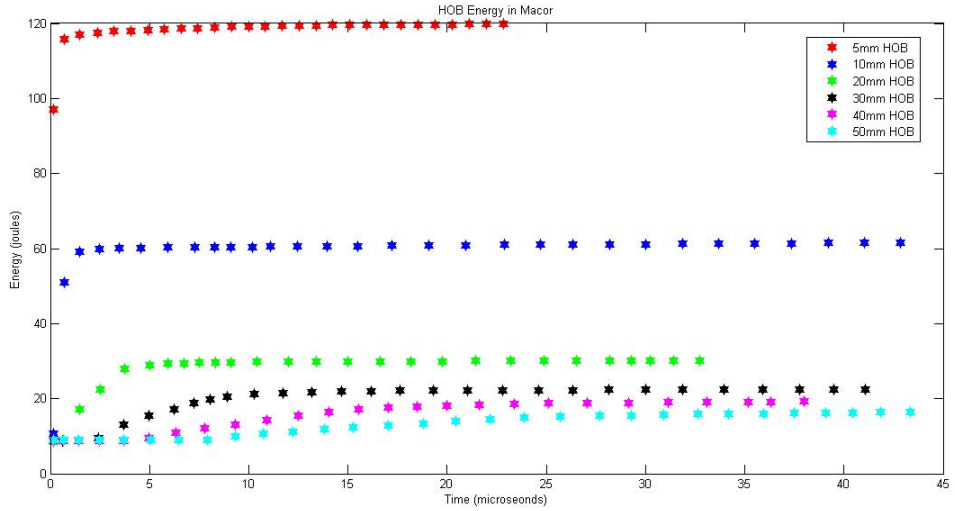

Figure 27. Energy in Macor block for several HOB shots

As expected, the energy decreases to a baseline as the height of burst increases. A similar relationship should also hold for the depth of burial shots. At the theoretical limit of an infinitely buried depth of burst, all the energy will remain within the Macor and none transmitted into the atmospheric gas mix. Figure 28 shows the energy contained within the Macor block as a function of time for the depth of burial calculations.

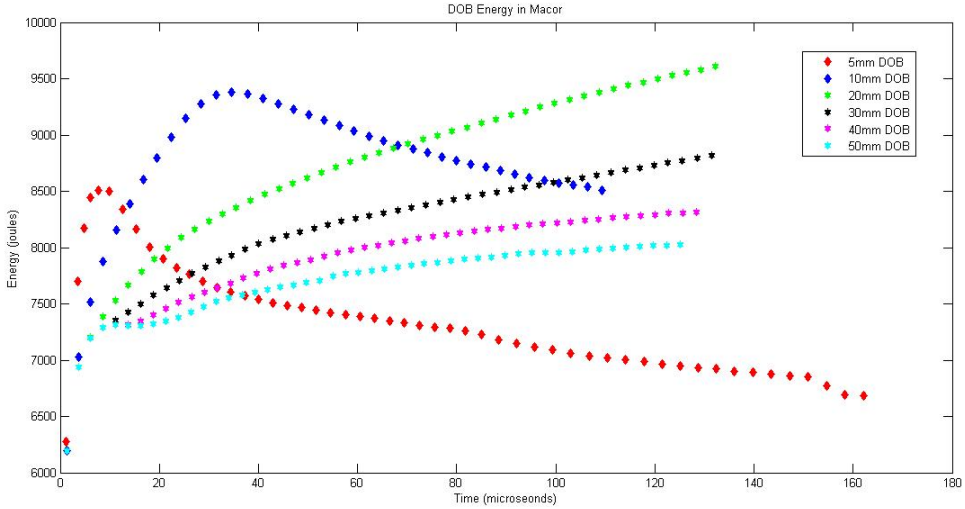

Figure 28. Energy in Macor block for several DOB shots

The total energy within the Macor increases from 5mm depth of burst to 10mm depth of burst, yet there is a noticeable difference between the profiles of the 5mm and 10mm DOB energies and the others. As the depth of burial increases beyond 20mm DOB, the energy begins to decline with depth of burst. At first glance, it may seem to indicate an error in the data, as the energy should increase to an asymptote, as the depth of burial gets deeper. Upon further investigation, using LLNL's visualization application, VisIT, it was discovered that for both the 5mm and 10mm depth of burial runs the exploding gas escapes the Macor block and leaves behind a crater. The point at which the Macor gives way corresponds to the two peaks in the total energy curve shown above for both the 5mm and 10mm DOB shots, as shown in Figure 28. Figure 29 shows a split view movie frame, with material on the right and pressure on the left, at 35 microseconds of the detonation. The breakout of the gold gas from the Macor block is clear. This breakout corresponds to the peak in the energy versus time plot in the Macor block for the 10mm DOB shot.

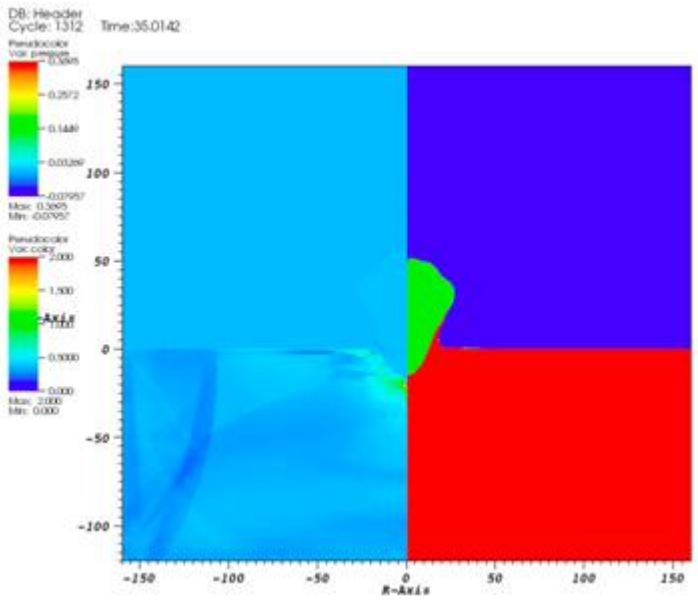

Figure 29. Split view of Material and Pressure at 35 microseconds for 10mm DOB shot

For all shots below 10mm, the fireball never escapes the Macor block, but simply bulges the “ground” where the fireball is forming. Figure 30 shows that the gold gas never escapes the Macor block by 120 microseconds for a 20mm depth of burial simulation.

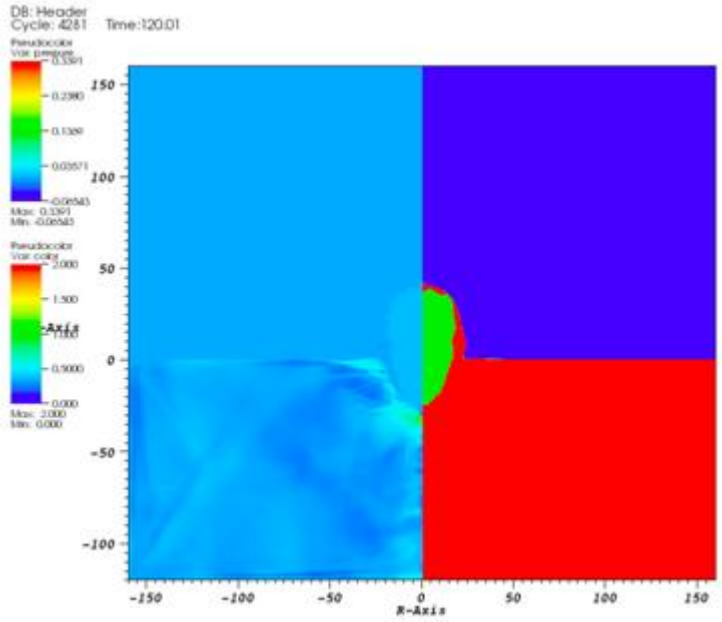

Figure 30. Split view of Material and Pressure at 120 microseconds for 20mm DOB shot

As demonstrated in Figures 30 and 31, the layer of Macor surrounding the gold gas becomes thicker as the depth of burial increases.

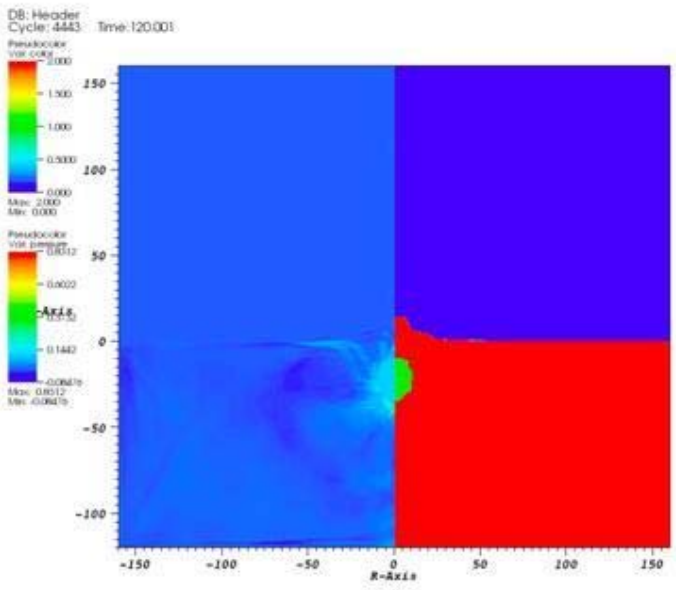

Figure 31. Split view of Material and Pressure at 120 microseconds for 30mm DOB shot

Thus, for 20mm and lower depths of burial, the energy contained within the gold gas fireball was added to the total energy of the Macor block, and with this addition, the total energy asymptotes as expected. The baseline energy of the Macor, due to its mass energy, was subtracted from each to show that the energy asymptotes to the 10kJ value of total deposited energy. Figure 32 illustrates the results of this corrected calculation of energy in the Macor block.

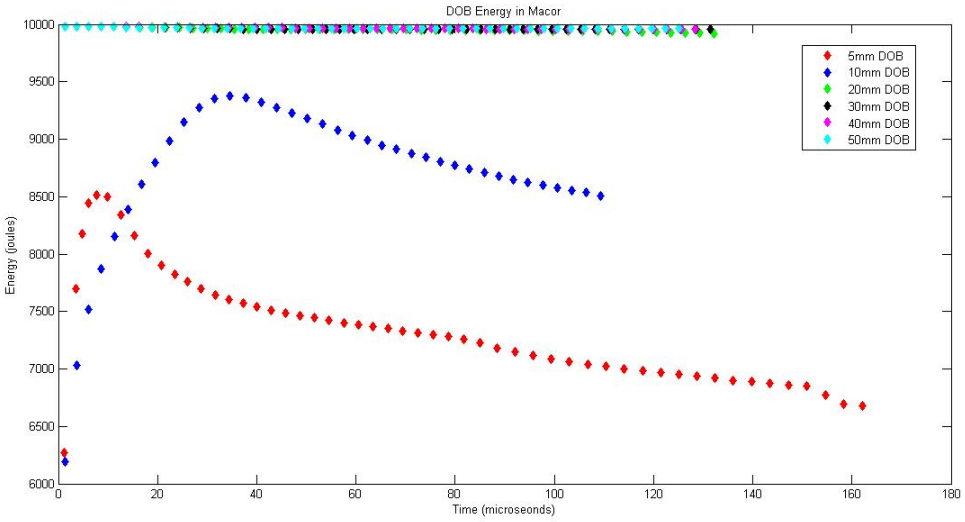

Figure 32. Corrected Plot of Energy in Macor block for several DOB shots

With the corrected energy-time plots for both height of burst and depth of burial runs, the peak energy values were plotted as a function of depth of burial in Figure 33 in order to construct the more familiar energy coupling curve.

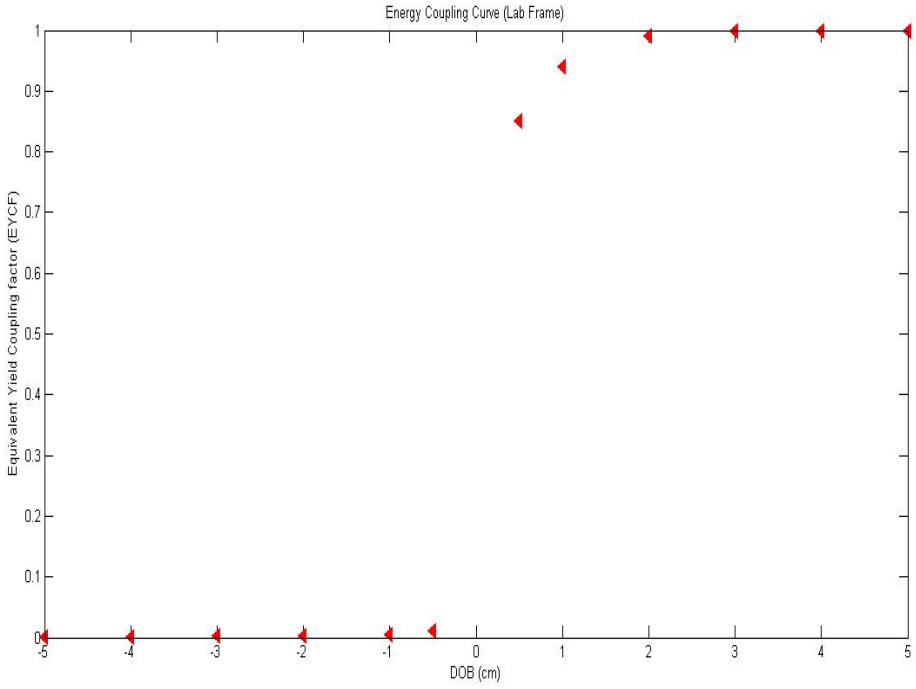

Figure 33. Lab Frame Energy Coupling Curve

In this plot, the ordinate corresponds to the energy coupling yield factor (ECYF), which is simply the peak energy in the Macor divided by the total input energy of 10kJ. A zero ECYF would correspond to an infinite high height of burst detonation and an ECYF of one would correspond to an infinitely deep depth of burial detonation. The abscissa indicates depth of burial where negative values along this axis correspond to the heights of burst for above-ground detonations. One key aspect of these data is that they are scalable. In order to scale up from the lab frame, in units of millimeters and kilojoules, the cube root scaling law, explained earlier in Chapter II sub-section B, "Scaling," was used to convert the straight depth of burial to a scaled depth of burial with units of distance per yield energy$^{1/3}$. The conversion factor shown below takes advantage of the cube root scaling law noted by Glasstone and Dolan.

Conversion factor:

$$1kJ = 2.383*10^{-13}\,MT \text{ (megaton)}$$
$$(1kJ)^{1/3} = (2.383*10^{-13})^{1/3} = 61.99*10^{-6}\,MT^{1/3}$$
$$1mm = 0.001m$$
$$1mm/1kJ^{1/3} = 0.001m/(61.99*10^{-6}\,MT^{1/3}) = 16.13m/MT^{1/3}$$

Each of the depth of burial/ height of burst was scaled up to a scaled depth of burial/ scaled height of burst using the conversion factor. How each distance was scaled is shown below, using the 5mm depth of burial case as an example.

$$\text{simulation depth of burial/ yield}^{1/3} * \text{ conversion factor = scaled depth of burial}$$
$$5mm/10kJ^{1/3} * (16.13m/MT^{1/3})/(1mm/1kJ^{1/3}) = 37.36m/MT^{1/3}$$

Table 5 shows the results of similar calculations for each depth of burial ranging from 5mm to 50 mm with a 10kJ yield.

mm /10kJ$^{1/3}$	m /MT$^{1/3}$
5	37.36
10	74.7
20	149.45
30	224.18
40	298.9
50	373.64

Table 5. Scaled Depth of Burial

Figure 34 shows the energy-coupling curve scaled to the world frame.

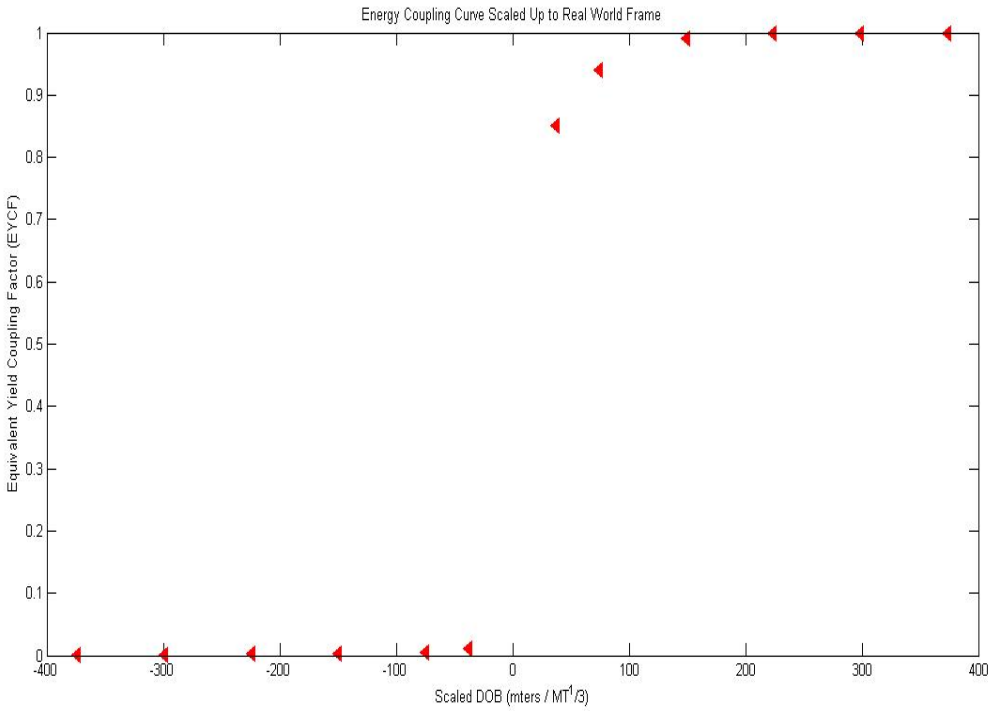

Figure 34. World Frame Energy Coupling Curve

The data can now be mapped to earlier calculations of explosions in various hard rock media made by several researchers and summarized by L. Glenn at LLNL in Figure 35. Those calculations are focused in the regime where there is strong coupling between the ground and air shock.

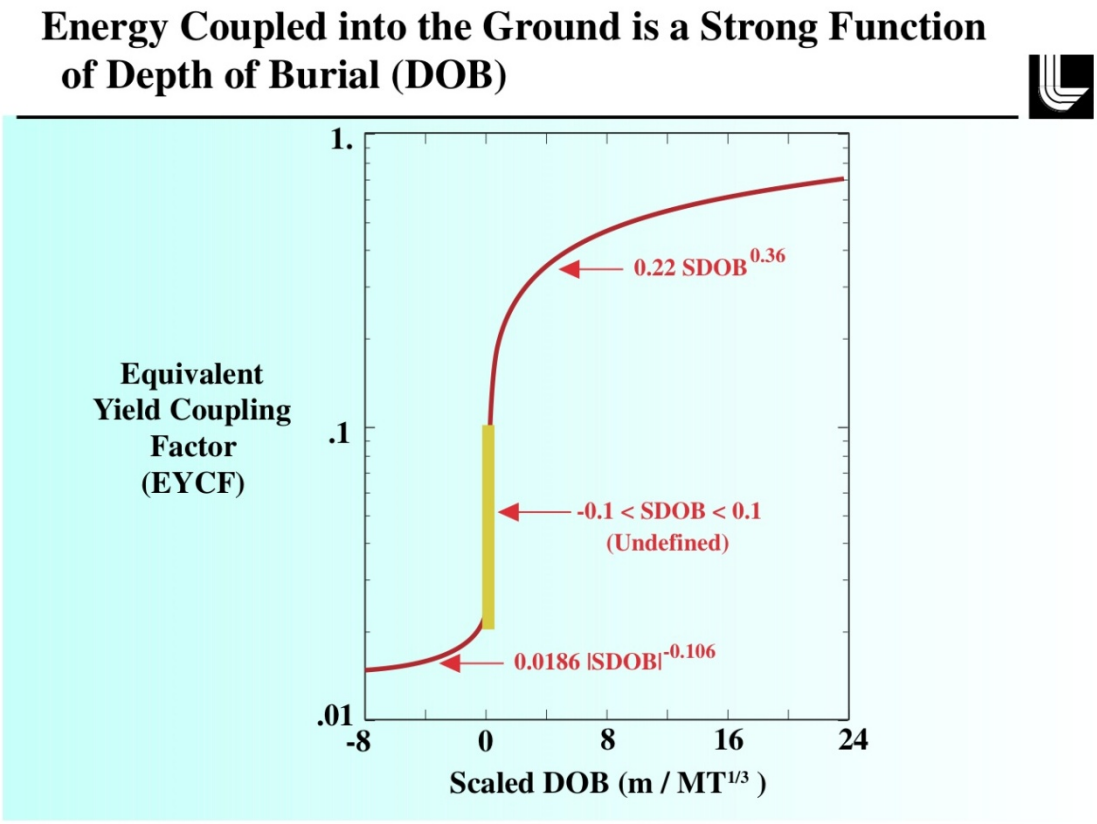

Figure 35. Energy Coupling Curve for Hard Rock From L.Glenn, 2002, p.16

First, the upper limit of the data fit was calculated by using the equation from the depth of burial data fit in Figure 35, setting the equivalent yield coupling factor (ECYF) to unity, and calculating the scaled depth of burial that corresponds to full coupling, i.e., no energy transmitted into air shock.

$$1 = 0.22 * \text{scaled depth of burial (SDOB)}^{0.36}$$
$$\ln(1/0.22) = 0.36 * \ln(SDOB)$$
$$\ln(SDOB) = (1/0.36) * \ln(1/0.22)$$
$$SDOB = e^{1/0.36*\ln(1/0.22)} = 67.08[m/MT^{1/3}]$$

This shows, according to the data fit, that all shots conducted at a scaled depth of burial greater than 67.08 m/ $MT^{1/3}$ represent a situation in which all of the energy would be fully coupled into the ground. Using the scaled depth of burial points from Table 2 and the data fit formulas summarized by L. Glenn, the ECYF data points from the numerical simulation was plotted against the coupling

curve of the hard rock data in order to show the correlation with the Macor simulation model. Figure 36 shows that within the limits of the data fit model, both the simulation and the hard rock model data fit agree within a margin of 5%. The red triangular points are from the simulation data for the various HOB/DOB calculations. The green curve is a plot of the two formulas from the hard rock data equations.

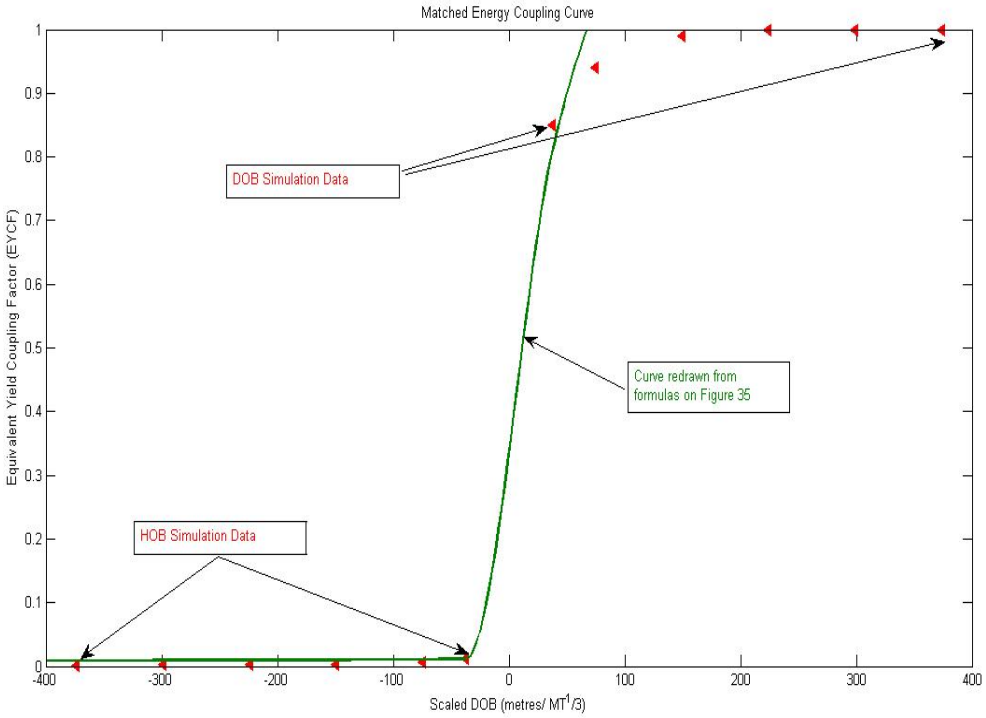

Figure 36. Matched Coupling Curve

Table 6 shows the EYCF for each of the 12 simulation calculations. The EYCF was calculated by taking the peak energies, from Figures 27 and 32, for the corresponding height of burst and depth of burial calculations respectively, and then dividing that value by the 10kJ input energy. So, for example, in the 10mm DOB calculation the maximum energy contained within the Macor was 9.4kJ which corresponds to the peak of the 10mm curve in Figure 32. This value of 9.4kJ was then divided by the 10kJ yield to result in an ECYF of 0.94.

Depth of Burial/ Height of Burst	Equivalent Yield Coupling Factor
5mm	.85
10mm	.94
20mm	.99
30mm	.99
40mm	.99
50mm	.99
-5mm (Height of Burst)	.012
-10mm	.006
-20mm	.003
-30mm	.0025
-40mm	.002
-50mm	.0018

Table 6. Equivalent Yield Coupling Factor from simulation data

Table 7 shows a similar data chart, the difference being that the scaled depths of burial/ heights of burst (shown in Table 5) were used along with the two equations from the hard rock data for both the height of burst and depth of burial to calculate the EYCF.

Scaled DOB/ Scaled HOB [m/MT$^{1/3}$]	Equivalent Yield Coupling Factor
37.36	.81
74.7	SDOB larger than 67.08 →1
149.45	SDOB larger than 67.08 →1
224.18	SDOB larger than 67.08 →1
298.9	SDOB larger than 67.08 →1
373.64	SDOB larger than 67.08 →1
-37.36 (Height of Burst)	.012 (**outside data range yet agrees)
-74.7	.011 (outside data range)
-149.45	.010 (outside data range)
-224.18	.010 (outside data range)
-298.9	.010 (outside data range)
-373.64	.009 (outside data range)

Table 7. Equivalent Yield Coupling Factor from live data fit curves

The range in which both the simulation data and the hard rock data overlap is small, yet within that range both the simulation and hard rock data agree to within 5%. Even slightly beyond the limits of the curve fit from the hard rock data both the simulation and it agree, as noted in the 5mm HOB (-37.36 m/MT$^{1/3}$ scaled HOB), where both the simulation and the hard rock data fit predict the exact same ECYF of .012.

THIS PAGE INTENTIONALLY LEFT BLANK

VII. CONCLUSION

Scaled simulation and computer modeling of nuclear weapon effects will play a significant role in the maintenance of the SBSSP. The National Ignition Facility at LLNL provides a unique opportunity to investigate nuclear weapon effects and the physics of nuclear weapons in support of the achievement of goals put forth by the NNSA and the SBSSP. This work provides information in evaluating the hydrodynamic response of materials to nuclear detonations at or near the earth's surface, which is a major component of the SPSSP agenda. The work presented in this thesis serves two purposes: first, to assist in the planning of the placement of shock sensors within a Macor object that will be used as a platform for upcoming NIF experiments designed to study the energy coupling/partitioning of a low yield nuclear detonation at or near the earth's surface; and second, to develop a basic set of computational data for development of a coupling curve. The coupling curve derived here, though partly based on an idealistic buried device, has proven to be very consistent with calculations of previous explosions in various hard rock media supported by limited test data. The coupling curve derived here and the supporting calculations serve as a basic set of data for further investigation of buried nuclear devices. Using the work done in this thesis, opportunities for further research include adding the effect of radiation to the simulations and altering the design of the Macor object to more closely model an inhomogeneous material.

THIS PAGE INTENTIONALLY LEFT BLANK

APPENDIX A

Appendix A is the input file for a 10mm height of burst calculation. Many of the original marker files have been removed for the purpose of saving paper. This should help clarify particular portions of the text, specifically the topics of boundary conditions and equations of state. This input file was called into the GEODYN executable and the results analyzed with both MATLAB and VisIT.

```
% units are specified in millimeters, milligrams, microseconds (GPa, km/s)

%%%%%%%%%%%%%%%%%%%%%%%%%
%%%% DEFINITIONS %%%%%%%
%%%%%%%%%%%%%%%%%%%%%%%%%
HOB=10 % height of burst

%%%%%%%%%%%%%%%%%%%%%%%%%
%% GLOBAL PARAMETERS %%
%%%%%%%%%%%%%%%%%%%%%%%%%
max_step = 100000
stop_time = 200

%%%%%%%%%%%%%%%%%%%%%%%%%
%%% DOMAIN GEOMETRY %%%
%%%%%%%%%%%%%%%%%%%%%%%%%
geometry:(
  % cylindrical (r-z) coordinates
  coord_sys = 1
  % low boundaries of (r,z) in domain
  prob_lo = [ 0   -120 ]
  % high boundaries of (r,z) in domain
  prob_hi = [ 160 160 ]
)

%%%%%%%%%%%%%%%%%%%%%%%%%
%%%%%% MESH/OUTPUT %%%%%%
%%%%%%%%%%%%%%%%%%%%%%%%%
amr:(
  % number of elements in (r,z) on base grid
  n_cell = [ 80 140 ]
```

```
% verbose output
v = 1
% verbose timestep output
v_step = 1
% maximum level of refinement
max_level = 2

% regrid interval (timesteps)
regrid_int = 2
% maximum grid size
max_grid_size = 32
% refinement ratio (per level)
ref_ratio = [4 4 4 4 4]
% number of extra cells around a grid to refine (per level)
n_error_buf = [1 2 1 1 1]

% root name of restart files
check_file = sesAucheck
% restart file interval (steps)
check_int = 100

% root name of plot files
plot_file = sesAuPlot
% plot file interval (steps) [cannot be specified with plot_per]
%plot_int = 100
% plot file period (microseconds) [cannot be specified with plot_int]
plot_per = 1
% plot variables (see RULESETS)
plot_vars = [ pressure density color vr vz sound_speed internal_energy
bulking_porosity pressure_cutoff friction_slope T11 T22 T33 T12 temperature ]

% marker specifications [ name (l)agrange/(e)ulerian r z ]
Markers = [
        [ pgauge1    e   86.0    50.0 ]
        [ pgauge2    e   130.0   75.0 ]
        [ pgauge3    e   140.0   25.0 ]
        [ gpgauge2   l   0.5     -70.0 ]
        [ gpgauge1   l   35.0    -35.0 ]
        [ gpgauge3   l   70.0    -70.0 ]




]
% marker output interval (steps)
```

```
  marker_int =  1
  % marker file write interval (steps)
  marker_dump_int =  100
  % marker variables (see RULESETS)
  marker_vars =  [ m_pressure m_density m_vel_mag m_vr m_vz m_T11 m_T22
m_T33 m_T12 m_color m_temperature m_internal_energy m_soundspeed
m_plastic_strain m_Tmin m_rdisp m_zdisp ]
)


%%%%%%%%%%%%%%%%%%%%%%%%%
%%% PHYSICS/SOLVER %%%%
%%%%%%%%%%%%%%%%%%%%%%%%%
hyp:(
  % number of materials
  n_materials=5
  % verbosity
  v = 0
  % minimum timestep below which to halt
  dt_cutoff = 0.00001
  % Courant stability factor
  cfl = .3
  % initial scale factor for timestep
  init_shrink = .01
  % maximum timestep increase per cycle
  change_max = 1.1
  % gravitational acceleration
  gravity = 0.

  % interval to sum integrated quantities
  sum_interval    =  100
  % integrated quantity variables (see RULESETS)
  integrated_quantities      =      [      sum_mass_source      sum_energy_source
sum_mass_source2              sum_energy_source2              sum_mass_source0
sum_energy_source0 ]

  % write integrated quantities file on restart
  %integrate_on_restart=1
)

%%%%%%%%%%%%%%%%%%%%%%%%%
% PROBLEM CONDITIONS %%
%%%%%%%%%%%%%%%%%%%%%%%%%
Prob:(
  % materials (see MATERIALS)
```

```
  materials=[ gas_mix_LEOS Au_LEOS Macor Air_LEOS Fe_LEOS ]
  % boundary condition types
  %% 0 = Interior/Periodic  2 = Outflow  %%
  %% 1 = Inflow             3 = Symmetry %%
  bc:lo:type = [ 3 1 ]
  bc:hi:type = [ 1 1 ]

  % inflow boundary specifications
  %% material is 0-indexed, density in g/cc, energy in kJ/g
  bc:lo:1:(
    material=3
    rho=0.0001
    e=0.52
  )
  bc:hi:0:(
    material=3
    rho=0.0001
    e=0.52
  )
  bc:hi:1:(
    material=3
    rho=0.0001
    e=0.52
  )
)

% Specifies that displacement variables should be stored
celldata<CellData>:(
  ops:[
    <CellDisplacement>=0
  ]
)

%%%%%%%%%%%%%%%%%%%%%%%%
%%%% CONFIGURATION %%%%
%%%%%%%%%%%%%%%%%%%%%%%%
Config:(
  % List of region names
  %% Specified order that regions are painted in.
  %% Last region fills remaining space.
  Regions = [ source  air_cone steel_cone ceramic
              ring atmosphere ceramic_shell air ]

  % Region specifications
  %% material is 0-indexed, density in g/cc, energy in kJ/g
```

```
Region:(
  % source
  %% 10kJ in 2mg of material, sphere of diameter 2mm
  source:(
    % expanded iron
    material = 1
    rho = 0.4774648
    e = 5e+3
    file = circle512
    % no scaling, translate in +y by height of burst
    Transform =  [ scale 1. 1. translate 0. `$:HOB` ]
  )

  % air inside cone
  air_cone:(
    % air
    material = 3
    rho = 0.0001
    e = 0.52
    % r-z pairs specifying polygon (r-z projection of cone)
    Points = [
      [ 0 `$:HOB+1000`]
      [ `0.6+1000/6`  `$:HOB+1001`]
      [ 0.6 `$:HOB+1` ]
      [ 0. `$:HOB` ]
    ]
  )

  % steel cone
  steel_cone:(
    % iron at reference density and energy
    material = 4
    % r-z pairs specifying polygon (r-z projection of outer cone)
    Points = [
      [ `0.4+1000/6`  `$:HOB+1001`]
      [ 0.4 `$:HOB+1` ]
      [ 0.6 `$:HOB+1` ]
      [ 1.4 `$:HOB+1.8` ]
      [ `1.4+1000/6`  `$:HOB+1001.8`]
    ]
  )

  % macor
  ceramic:(
    % macor at reference density
```

```
  material =  2
  e = 0.0000405
  Points = [
    [ 0      -100 ]
    [ 100    -100 ]
    [ 100    0.06 ]
    [ 0      0.06 ]
  ]
)

% macor ring
ring:(
  % macor at reference density
  material =  2
  e = 0.0000405
  Points = [
    [ 100.5       -10 ]
    [ 149.5       -10 ]
    [ 150.      0.06 ]
    [ 100.      0.06 ]
  ]
)

% gas-mixture atmosphere
atmosphere:(
  % gas mixture
  material = 0
  rho=0.00153
  temperature = 310
  % composition of mixture
  "qq[0]" = 0.65
  "qq[1]" = 0.20
  "qq[2]" = 0.10
  "qq[3]" = 0.05
  Points = [
    [ 0   -100 ]
    [ 150 -100 ]
    [ 150 150 ]
    [ 0 150 ]
  ]
)

% macor shell
ceramic_shell:(
  % macor at reference density
```

```
      material = 2
      e = 0.0000405
      Points = [
        [ 0       -105 ]
        [ 155     -105 ]
        [ 155      155 ]
        [ 0        155 ]
        [ 0        150 ]
        [ 150      150 ]
        [ 150     -100 ]
        [ 0       -100 ]
      ]
    )

    % remaining air
    air:(
      % air
      material = 3
      rho = 0.0001
      e = 0.52
    )
  )
)

%%%%%%%%%%%%%%%%%%%%%%%%
%%% REFINEMENT RULES %%
%%%%%%%%%%%%%%%%%%%%%%%%
% Specifies refinement condition
refinement<Tagger>:(
  % refine on material interfaces and pressure gradients
  logic<SymbolFunction>:(
    f="(interfaces|pressure)"
    variable="interfaces,pressure"
  )

  % refinement variables (see RULESETS)
  derive=[ref_color ref_p ]

  % material interface detection
  %% refine when "color" is not an integer
  interfaces<FabFunction>:(
    comp=[ref_color]
    f=abs_remainder_offset parameters=[1.e-8]
  )
```

```
  % pressure gradient detection
  %% refine when relative difference (pA - pB)/(min(pA,pB,pMin)) > 0.3
  %% where pMin = 0.0002GPa
  pressure<FabFunction>:(
    comp=[ref_p]
    f=relative_gradient_offset parameters=[0.0002 .3]
  )

)

%%%%%%%%%%%%%%%%%%%%%%%%
%%%%%%% RULESETS %%%%%%%%
%%%%%%%%%%%%%%%%%%%%%%%%

% plot variables (rules must match names)
pressure<DeriveRuleSet>:(
  models=[ StressTensor Energies ]
  rules:[
    <Rule>:(var=p averager=bulk_modulus_average)
    <Rule>:(var=rho averager=volume_average)
    <Rule>:(var=material_number averager=volume_average)
    <Rule>:(var="v[0]" )
    <Rule>:(var="v[1]" )
    <Rule>:(var=c)
    <Rule>:(var=e)
    <Rule>:(var=bulking_porosity )
    <Rule>:(var=pressure_cutoff )
    <Rule>:(var=friction_slope)
    <Rule>:(var="T[T11]" )
    <Rule>:(var="T[T22]" )
    <Rule>:(var="T[T33]" )
    <Rule>:(var="T[T12]" )
    <Rule>:(var=temperature)
  ]
)

% marker variables (rules must match names)
m_pressure<DeriveRuleSet>:(
  models=[StressTensor Energies ]
  rules:[
    <Rule>:(var=p averager=bulk_modulus_average)
    <Rule>:(var=rho averager=volume_average)
    <Rule>:(var=v_mag)
    <Rule>:(var="v[0]" )
    <Rule>:(var="v[1]" )
```

```
      <Rule>:(var="T[T11]")
      <Rule>:(var="T[T22]")
      <Rule>:(var="T[T33]")
      <Rule>:(var="T[T12]")
      <Rule>:(var=material_number averager=volume_average)
      <Rule>:(var=temperature)
      <Rule>:(var=e)
      <Rule>:(var=c)
      <Rule>:(var=plastic_strain)
      <Rule>:(var=Tminhistory)
      <Rule>:(var="displacement[0]")
      <Rule>:(var="displacement[1]")
   ]
)

% integrated quantities variables (rules must match names)
sum_mass_source<DeriveRuleSet>:(
   models = [ Energies ]
   rules:[
      <Rule>:(var=rho averager=volume_sum materials=[1])
      <Rule>:(var=e_tot averager=mass_sum materials=[1])
      <Rule>:(var=rho averager=volume_sum materials=[2])
      <Rule>:(var=e_tot averager=mass_sum materials=[2])
      <Rule>:(var=rho averager=volume_sum materials=[0])
      <Rule>:(var=e_tot averager=mass_sum materials=[0])
   ]
)

% refinement variables
ref_color<DeriveRuleSet>:(
      models=[EOS]
      rules:[
         <Rule>:(var=material_number averager=volume_average)
         <Rule>:(var=p averager=bulk_modulus_average)
      ]
)

%%%%%%%%%%%%%%%%%%%%%%%%
%%%%%%% MATERIALS %%%%%%%
%%%%%%%%%%%%%%%%%%%%%%%%
gas_mix_LEOS<Material>: (
   models: [
      <NoPorosityVariable> = 0
      <RhoSolid> = 0
      <N_GammaAveraged_EOS>:(
```

```
        EOS:[
          <LEOS> :( use_energy_offset=1 material_number=100 ) % qq[0] - Ne
          <LEOS> :( use_energy_offset=1 material_number=180 ) % qq[1] - Ar
          <LEOS> :( use_energy_offset=1 material_number=360 ) % qq[2] - Kr
          <LEOS> :( use_energy_offset=1 material_number=540 ) % qq[3] - Xe
        ]
      )
      <N_LimitFraction> = 0
      <SphericalStressTensor> = 0
      <ZeroShearModulus> = 0
      <Smooth_PressureCutOff>: (pmin=0)
      <ZeroFrictionSlope> = 0
      <Tminhistory> = 0
    ]
)

Air_LEOS<Material>: (
  models: [
    <NoPorosityVariable> = 0
    <RhoSolid> = 0
    <LEOS> :( material_number=2260 )
    <NoUpdate> = 0
    <SphericalStressTensor> = 0
    <ZeroShearModulus> = 0
    <Smooth_PressureCutOff>: (pmin=0)
    <ZeroFrictionSlope> = 0
    <Tminhistory>=0
  ]
)

Fe_LEOS<Material>: (
  models: [
    <NoPorosityVariable> = 0
    <RhoSolid> = 0
    <LEOS>: ( material_number=260 )
    <NoUpdate> = 0
    <SphericalStressTensor> = 0
    <ZeroShearModulus> = 0
    <Smooth_PressureCutOff>: (pmin=0)
    <ZeroFrictionSlope> = 0
    <Tminhistory>=0
  ]
)
Au_LEOS<Material>: (
  models: [
```

```
    <NoPorosityVariable> = 0
    <RhoSolid> = 0
    <LEOS>: ( material_number=2700 leos_name=/usr/gapps/data/eos/sesame )
    <NoUpdate> = 0
    <SphericalStressTensor> = 0
    <ZeroShearModulus> = 0
    <Smooth_PressureCutOff>: (pmin=0)
    <ZeroFrictionSlope> = 0
    <Tminhistory>=0
  ]
)


Macor<Material>: (
  models: [
    <ElasticPorosityVariable> = 0
    <RhoSolid> = 0
    <MieGruneisen_EOS>: (
      rho0 = 2.52
      c0   = 4.58
      s1   = 1.4
      s2   = 0.
      s3   = 0.
      g = 1.
      b = 0.
    )
    <HistoryDependent_PressureCutOff>: ( pmin=-0.008 )
    <PoreElasticity>: ( a=0. b=1. )
    <PseudoCapYieldStrength1>:(
      scale_factor=1.
      Y_c=0.345
      Y_t=0.1
      tau_dam=0.00001
      P_hard_rate=5.
      P_hard_exp=0.5
      Yrat=0.98
      cap0=0.5
      cap00=0.5
      cap_power=2.
      strain_hard_eps=0.02
      strain_tofail=0.0001
      soft_rate=5.
      rate_function<SymbolicFunction>: ( function="(x+1.)^0.12" )
      residual_function<SymbolicFunction>: ( function="1.*x" )
    )
```

```
    <PseudoCapCompaction>:(
      poro0=0.001
      mu_c0=10.
      slope0=0.1
      bulking_k1<SymbolicFunction>: ( function="0.05*x" )
      tau_comp=0
    )
    <RateDependentFunctionPlasticUpdatewithCorrection>:(
      tau_of_p<Const>: ( f=0 )
    )
    <ElasticUpdate1> = 0
    <YieldLodeAngleTerm>: ( q20 = 0.5 function<Const>:(f=1) )
    <Stress> = 0
    <ConstantPoissonRatio>: ( nu=0.29 )
    <PseudoCapBulkingwithCorrection> = 0
    <PseudoCapBulkingCorrection>: (
      k1=0.5
      k=0.5
    )
    <FrictionSlope>: ( y0=1.5 )
  ]
)
```

APPENDIX B

Appendix B is the input file for the modified 30mm depth of burial calculation. Many of the original marker files have been removed for the purpose of saving paper. The original goal of the modified DOB set up was to have a layer of air around both the Macor and the gas-mix, but without a solid boundary between the two gases the gas-mix expanded to fill the problem space. This setup worked also as it still left a single material at the problem boundary, which eliminated the reflected wave noise, as shown in Figures 17 and 18. This input file was called into the GEODYN executable and the results analyzed with both MATLAB and VisIT.

```
% units are specified in millimeters, milligrams, microseconds (GPa, km/s)

%%%%%%%%%%%%%%%%%%%%%%%%%%
%%%%% DEFINITIONS %%%%%%%
%%%%%%%%%%%%%%%%%%%%%%%%%%
HOB=-30 % depth of burst

%%%%%%%%%%%%%%%%%%%%%%%%%%
%% GLOBAL PARAMETERS %%
%%%%%%%%%%%%%%%%%%%%%%%%%%
max_step = 100000
stop_time = 200

%%%%%%%%%%%%%%%%%%%%%%%%%%
%%% DOMAIN GEOMETRY %%%
%%%%%%%%%%%%%%%%%%%%%%%%%%
geometry:(
  % cylindrical (r-z) coordinates
  coord_sys = 1
  % low boundaries of (r,z) in domain
  prob_lo = [ 0   -120 ]
  % high boundaries of (r,z) in domain
  prob_hi = [ 160 160 ]
)

%%%%%%%%%%%%%%%%%%%%%%%%%%
%%%%%% MESH/OUTPUT %%%%%%
%%%%%%%%%%%%%%%%%%%%%%%%%%
amr:(
```

```
% number of elements in (r,z) on base grid
n_cell = [ 80 140 ]
% verbose output
v = 1
% verbose timestep output
v_step = 1
% maximum level of refinement
max_level = 2

% regrid interval (timesteps)
regrid_int = 2
% maximum grid size
max_grid_size = 32
% refinement ratio (per level)
ref_ratio = [4 4 4 4 4]
% number of extra cells around a grid to refine (per level)
n_error_buf = [1 2 1 1 1]

% root name of restart files
check_file = chk
% restart file interval (steps)
check_int = 200

% root name of plot files
plot_file = plt
% plot file interval (steps) [cannot be specified with plot_per]
%plot_int = 100
% plot file period (microseconds) [cannot be specified with plot_int]
plot_per = 1
% plot variables (see RULESETS)
plot_vars = [ pressure density color vr vz sound_speed internal_energy
bulking_porosity pressure_cutoff friction_slope T11 T22 T33 T12 temperature ]

% marker specifications [ name (l)agrange/(e)ulerian r z ]
Markers = [
        [ pgauge1    e   86.0    50.0 ]
        [ pgauge2    e   130.0  75.0 ]
        [ pgauge3    e   25.0    140.0 ]
        [ gpgauge2   l   0.5     -70.0 ]
        [ gpgauge1   l   35.0    -35.0 ]
        [ gpgauge3   l   70.0    -70.0 ]
```

```
  ]
  % marker output interval (steps)
  marker_int =  1
  % marker file write interval (steps)
  marker_dump_int =  100
  % marker variables (see RULESETS)
  marker_vars =  [ m_pressure m_density m_vel_mag m_vr m_vz m_T11 m_T22
m_T33 m_T12 m_color m_temperature m_internal_energy m_soundspeed
m_plastic_strain m_Tmin m_rdisp m_zdisp ]
)


%%%%%%%%%%%%%%%%%%%%%%%%
%%% PHYSICS/SOLVER %%%%
%%%%%%%%%%%%%%%%%%%%%%%%
hyp:(
  % number of materials
  n_materials=4
  % verbosity
  v = 0
  % minimum timestep below which to halt
  dt_cutoff = 0.00001
  % Courant stability factor
  cfl = .2
  % initial scale factor for timestep
  init_shrink = .01
  % maximum timestep increase per cycle
  change_max = 1.1
  % gravitational acceleration
  gravity = 0.

  % interval to sum integrated quantities
  sum_interval    =  100
  % integrated quantity variables (see RULESETS)
  integrated_quantities        =        [    sum_mass_source    sum_energy_source
sum_mass_source2              sum_energy_source2              sum_mass_source0
sum_energy_source0 ]
  % write integrated quantities file on restart
  %integrate_on_restart=1
)

%%%%%%%%%%%%%%%%%%%%%%%%
% PROBLEM CONDITIONS %%
%%%%%%%%%%%%%%%%%%%%%%%%
Prob:(
```

```
  % materials (see MATERIALS)
  materials=[ gas_mix_LEOS Au_LEOS Macor Air_LEOS ]

  % boundary condition types
  %% 0 = Interior/Periodic  2 = Outflow  %%
  %% 1 = Inflow             3 = Symmetry %%
  bc:lo:type = [ 3 1 ]
  bc:hi:type = [ 1 1 ]

  % inflow boundary specifications
  %% material is 0-indexed, density in g/cc, energy in kJ/g
  bc:lo:1:(
    material=3
    rho=0.0001
    e=0.52
  )
  bc:hi:0:(
    material=3
    rho=0.0001
    e=0.52
  )
  bc:hi:1:(
    material=3
    rho=0.0001
    e=0.52
  )
)

% Specifies that displacement variables should be stored
celldata<CellData>:(
  ops:[
    <CellDisplacement>=0
  ]
)

%%%%%%%%%%%%%%%%%%%%%%%%
%%%% CONFIGURATION %%%%
%%%%%%%%%%%%%%%%%%%%%%%%
Config:(
  % List of region names
  %% Specified order that regions are painted in.
  %% Last region fills remaining space.
  Regions = [ source ceramic atmosphere ]

  % Region specifications
```

```
%% material is 0-indexed, density in g/cc, energy in kJ/g
Region:(
  % source
  %% 10kJ in 2mg of material, sphere of diameter 2mm
  source:(
    % expanded gold
    material = 1
    rho = 0.4774648
    e = 5e+3
    file = circle512
    % no scaling, translate in +y by height of burst
    Transform =  [ scale 1. 1. translate 0. `$:HOB` ]
  )

  % macor
  ceramic:(
    % macor at reference density
    material =  2
    e = 0.0000405
    Points = [
      [ 0      -110 ]
      [ 150    -110 ]
      [ 150    0.06 ]
      [ 0      0.06 ]
    ]
  )

  % gas-mixture atmosphere
  atmosphere:(
    % gas mixture
    material = 0
    rho=0.00153
    temperature = 310
    % composition of mixture
    "qq[0]" = 0.65
    "qq[1]" = 0.20
    "qq[2]" = 0.10
    "qq[3]" = 0.05
    Points = [
      [ 0   0.06 ]
      [ 0   150 ]
      [ 150 150 ]
      [ 150 0.06 ]
    ]
  )
```

```
    % air boundary
     air:(
       % air boundary
       material =  3
       e = 0.52
         rho=0.0001
     )


  )
)

%%%%%%%%%%%%%%%%%%%%%%%%
%%% REFINEMENT RULES %%
%%%%%%%%%%%%%%%%%%%%%%%%
% Specifies refinement condition
refinement<Tagger>:(
  % refine on material interfaces and pressure gradients
  logic<SymbolFunction>:(
    f="(interfaces|pressure)"
    variable="interfaces,pressure"
  )

  % refinement variables (see RULESETS)
  derive=[ref_color ref_p ]

  % material interface detection
  %% refine when "color" is not an integer
  interfaces<FabFunction>:(
    comp=[ref_color]
    f=abs_remainder_offset parameters=[1.e-8]
  )

  % pressure gradient detection
  %% refine when relative difference (pA - pB)/(min(pA,pB,pMin)) > 0.3
  %% where pMin = 0.0002GPa
  pressure<FabFunction>:(
    comp=[ref_p]
    f=relative_gradient_offset parameters=[0.0002 .3]
  )

)

%%%%%%%%%%%%%%%%%%%%%%%%
%%%%%%% RULESETS %%%%%%%%
```

```
%%%%%%%%%%%%%%%%%%%%%%%%

% plot variables (rules must match names)
pressure<DeriveRuleSet>:(
  models=[ StressTensor Energies ]
  rules:[
    <Rule>:(var=p averager=bulk_modulus_average)
    <Rule>:(var=rho averager=volume_average)
    <Rule>:(var=material_number averager=volume_average)
    <Rule>:(var="v[0]" )
    <Rule>:(var="v[1]" )
    <Rule>:(var=c)
    <Rule>:(var=e)
    <Rule>:(var=bulking_porosity )
    <Rule>:(var=pressure_cutoff )
    <Rule>:(var=friction_slope)
    <Rule>:(var="T[T11]" )
    <Rule>:(var="T[T22]" )
    <Rule>:(var="T[T33]" )
    <Rule>:(var="T[T12]" )
    <Rule>:(var=temperature)
  ]
)

% marker variables (rules must match names)
m_pressure<DeriveRuleSet>:(
  models=[StressTensor Energies ]
  rules:[
    <Rule>:(var=p averager=bulk_modulus_average)
    <Rule>:(var=rho averager=volume_average)
    <Rule>:(var=v_mag)
    <Rule>:(var="v[0]" )
    <Rule>:(var="v[1]" )
    <Rule>:(var="T[T11]")
    <Rule>:(var="T[T22]")
    <Rule>:(var="T[T33]")
    <Rule>:(var="T[T12]")
    <Rule>:(var=material_number averager=volume_average)
    <Rule>:(var=temperature)
    <Rule>:(var=e)
    <Rule>:(var=c)
    <Rule>:(var=plastic_strain)
    <Rule>:(var=Tminhistory)
    <Rule>:(var="displacement[0]")
    <Rule>:(var="displacement[1]")
```

```
  ]
)

% integrated quantities variables (rules must match names)
sum_mass_source<DeriveRuleSet>:(
  models = [ Energies ]
  rules:[
    <Rule>:(var=rho averager=volume_sum materials=[1])
    <Rule>:(var=e_tot averager=mass_sum materials=[1])
    <Rule>:(var=rho averager=volume_sum materials=[2])
    <Rule>:(var=e_tot averager=mass_sum materials=[2])
    <Rule>:(var=rho averager=volume_sum materials=[0])
    <Rule>:(var=e_tot averager=mass_sum materials=[0])


  ]
)

% refinement variables
ref_color<DeriveRuleSet>:(
    models=[EOS]
    rules:[
      <Rule>:(var=material_number averager=volume_average)
      <Rule>:(var=p averager=bulk_modulus_average)
    ]
)

%%%%%%%%%%%%%%%%%%%%%%%%
%%%%%%% MATERIALS %%%%%%%
%%%%%%%%%%%%%%%%%%%%%%%%
gas_mix_LEOS<Material>: (
  models: [
    <NoPorosityVariable> = 0
    <RhoSolid> = 0
    <N_GammaAveraged_EOS>:(
      EOS:[
        <LEOS> :( use_energy_offset=1 material_number=100 ) % qq[0] - Ne
        <LEOS> :( use_energy_offset=1 material_number=180 ) % qq[1] - Ar
        <LEOS> :( use_energy_offset=1 material_number=360 ) % qq[2] - Kr
        <LEOS> :( use_energy_offset=1 material_number=540 ) % qq[3] - Xe
      ]
    )
    <N_LimitFraction> = 0
    <SphericalStressTensor> = 0
    <ZeroShearModulus> = 0
```

```
    <Smooth_PressureCutOff>: (pmin=0)
    <ZeroFrictionSlope> = 0
    <Tminhistory> = 0
  ]
)


Au_LEOS<Material>: (
  models: [
    <NoPorosityVariable> = 0
    <RhoSolid> = 0
    <LEOS>: ( material_number=2700 leos_name=/usr/gapps/data/eos/sesame )
    <NoUpdate> = 0
    <SphericalStressTensor> = 0
    <ZeroShearModulus> = 0
    <Smooth_PressureCutOff>: (pmin=0)
    <ZeroFrictionSlope> = 0
    <Tminhistory>=0
  ]
)
Air_LEOS<Material>:(
  models: [
        <NoPorosityVariable>=0
        <RhoSolid>=0
        <LEOS>:(material_number=2260)
        <NoUpdate>=0
        <SphericalStressTensor>=0
        <ZeroShearModulus>=0
        <Smooth_PressureCutOff>: (pmin=0)
        <ZeroFrictionSlope>=0
        <Tminhistory>=0
        ]
)




Macor<Material>: (
  models: [
    <ElasticPorosityVariable> = 0
    <RhoSolid> = 0
    <MieGruneisen_EOS>: (
      rho0 = 2.52
      c0   = 4.58
      s1   = 1.4
```

```
      s2   = 0.
      s3   = 0.
      g = 1.
      b = 0.
    )
    <HistoryDependent_PressureCutOff>: ( pmin=-0.008 )
    <PoreElasticity>: ( a=0. b=1. )
    <PseudoCapYieldStrength1>:(
      scale_factor=1.
      Y_c=0.345
      Y_t=0.1
      tau_dam=0.00001
      P_hard_rate=5.
      P_hard_exp=0.5
      Yrat=0.98
      cap0=0.5
      cap00=0.5
      cap_power=2.
      strain_hard_eps=0.02
      strain_tofail=0.0001
      soft_rate=5.
      rate_function<SymbolicFunction>: ( function="(x+1.)^0.12" )
      residual_function<SymbolicFunction>: ( function="1.*x" )
    )
    <PseudoCapCompaction>:(
      poro0=0.001
      mu_c0=10.
      slope0=0.1
      bulking_k1<SymbolicFunction>: ( function="0.05*x" )
      tau_comp=0
    )
    <RateDependentFunctionPlasticUpdatewithCorrection>:(
      tau_of_p<Const>: ( f=0 )
    )
    <ElasticUpdate1> = 0
    <YieldLodeAngleTerm>: ( q20 = 0.5 function<Const>:(f=1) )
    <Stress> = 0
    <ConstantPoissonRatio>: ( nu=0.29 )
    <PseudoCapBulkingwithCorrection> = 0
    <PseudoCapBulkingCorrection>: (
      k1=0.5
      k=0.5
    )
    <FrictionSlope>: ( y0=1.5 )
  ]
)
```

LIST OF REFERENCES

[1] R. Rowberg, The National Ignition Facility: Management, Technical, and Other Issues, RL30540, 1–3, (2001). http://www.policyarchive.org/handle/10207/bitstreams/1037.pdf. [Accessed January 10, 2010].

[2] "Stockpile Stewardship Program," September 29, 2004. [Online] Available: http://www.nv.doe.gov/library/factsheets/DOENV_1017.pdf. [Accessed July 22, 2009].

[3] "Science & Technology: A Legacy of Lasers," May 29, 2009 [Online] Available: https://lasers.llnl.gov/science_technology/. [Accessed June 17, 2009].

[4] S. Glasstone and P. Dolan, *The Effects of Nuclear Weapons.* Washington D.C.: U.S. Department of Defense and the Energy Research and Development Administration, 1977, pp. 63–80

[5] W. Chen and G. Ravichandran, "Dynamic Compressive Failure of a Glass Ceramic Under Lateral Confinement," *J. Mech. Phys. Solids*, vol. 45, pp. 1303–1328.

[6] B. Bonner, M. Bono, B. Dunlop, and K. Fournier, (2008). Energy-Partitioning Energy-Coupling (EPEC) Experiments [PowerPoint slides].

[7] "Piezoelectric Polymers," [Online] Available: http://ktech.com/featured_products/piezoelectric_polymers.cfm. [Accessed June 17, 2009].

[8] G. Barasch, "Light Flash Produced by an Atmospheric Nuclear Explosion," *Los Alamos Scientific Laboratory Mini Review*, vol. 79–84, pp. 2–4.

[9] M. Rubin, O. Vorobiev, and L. Glenn, "Mechanical and Numerical Modeling of a Porous Elastic-visoplastic Material with Tensile Failure," *International Journal of Solids and Structures*, vol. 37, pp. 1841–1871.

[10] L. Glenn, (2002). The Ensemble Model For Ground Shock In Hard Rock [PowerPoint slides].

[11] I. Lomov, R. Pember, J. Greenough, and B. Liu, "Patch-based Adaptive Mesh Refinement for Multimaterial Hydrodynamics," *Lawrence Livermoor National Laboratory*, UCRL-CONF-216444 pp. 3–12.

THIS PAGE INTENTIONALLY LEFT BLANK

INITIAL DISTRIBUTION LIST

1. Defense Technical Information Center
   Ft. Belvoir, Virginia

2. Dudley Knox Library
   Naval Postgraduate School
   Monterey, California